Neuron
Article

Erbb4 Deletion from Fast-Spiking Interneurons Causes Schizophrenia-like Phenotypes

Isabel del Pino,[1,4] Cristina García-Frigola,[1,4] Nathalie Dehorter,[1,5] Jorge R. Brotons-Mas,[1,5] Efrén Alvarez-Salvado,[1] María Martínez de Lagrán,[2] Gabriele Ciceri,[1] María Victoria Gabaldón,[3] David Moratal,[3] Mara Dierssen,[2] Santiago Canals,[1] Oscar Marín,[1,*] and Beatriz Rico[1,*]

[1]Instituto de Neurociencias, Consejo Superior de Investigaciones Científicas and Universidad Miguel Hernández, Sant Joan d'Alacant 03550, Spain

[2]Center for Genomic Regulation, Universitat Pompeu Fabra, and Centro de Investigación Biomédica en Red de Enfermedades Raras (CIBERER), Barcelona 08003, Spain

[3]Center for Biomaterials and Tissue Engineering, Universidad Politécnica de Valencia, 46022 Valencia, Spain

[4]These authors contributed equally to this work and are listed alphabetically

[5]These authors contributed equally to this work

*Correspondence: o.marin@umh.es (O.M.), brico@umh.es (B.R.)

http://dx.doi.org/10.1016/j.neuron.2013.07.010

SUMMARY

Genetic variation in neuregulin and its ErbB4 receptor has been linked to schizophrenia, although little is known about how they contribute to the disease process. Here, we have examined conditional *Erbb4* mouse mutants to study how disruption of specific inhibitory circuits in the cerebral cortex may cause large-scale functional deficits. We found that deletion of ErbB4 from the two main classes of fast-spiking interneurons, chandelier and basket cells, causes relatively subtle but consistent synaptic defects. Surprisingly, these relatively small wiring abnormalities boost cortical excitability, increase oscillatory activity, and disrupt synchrony across cortical regions. These functional deficits are associated with increased locomotor activity, abnormal emotional responses, and impaired social behavior and cognitive function. Our results reinforce the view that dysfunction of cortical fast-spiking interneurons might be central to the pathophysiology of schizophrenia.

INTRODUCTION

Schizophrenia is a complex neurodevelopmental syndrome caused by both genetic and environmental factors and characterized by a heterogeneous collection of symptoms that include altered perception, decreased motivation, and various cognitive deficits, such as attention and memory problems (Insel, 2010). Despite intensive research, little progress has been made in designing effective treatments for most of these symptoms, in particular for restoring emotional and cognitive functions (Minzenberg and Carter, 2012; Pratt et al., 2012). This is largely due to the fact that schizophrenia still lacks unequivocal diagnostic neuropathology and strong causative genetic mutations.

Postmortem studies suggest that schizophrenia is associated with deficits of gamma-aminobutyric acid (GABA) synaptic transmission in the cerebral cortex. Multiple lines of evidence indicate that parvalbumin-expressing (PV+), fast-spiking interneurons are predominantly affected in schizophrenia (Curley and Lewis, 2012; Lewis, 2011). In addition, postmortem studies suggest that the number of GABAergic synapses made by these interneurons is reduced in individuals with schizophrenia (Lewis et al., 2001; Woo et al., 1998). Because PV+ fast-spiking interneurons modulate oscillatory activity in the gamma-range (Buzsáki and Draguhn, 2004; Cardin et al., 2009; Sohal et al., 2009), and these oscillations play a prominent role in cognition (Jensen et al., 2007; Uhlhaas and Singer, 2012), it has been hypothesized that synaptic dysfunction of these neurons may contribute to the cognitive deficits observed in schizophrenia (Lewis et al., 2005; Lisman et al., 2008).

Converging evidence over several susceptibility genes is beginning to shed light on the mechanisms underlying the pathophysiology of schizophrenia (Allen et al., 2008; Mulle, 2012; Sullivan et al., 2012). One of these genes encodes ERBB4, a tyrosine kinase receptor that is highly expressed in the developing brain (Nicodemus et al., 2006; Norton et al., 2006; Silberberg et al., 2006; Walsh et al., 2008). ERBB4 binds molecules of the Neuregulin family, in particular NRG1 and NGR3, encoded by two additional schizophrenia susceptibility genes (Chen et al., 2009; Harrison and Law, 2006; Kao et al., 2010; Morar et al., 2011; Norton et al., 2006; Stefansson et al., 2002; Wang et al., 2008). In mice, neuregulin signaling regulates multiple aspects of neurodevelopment, including neuronal migration, axon guidance, myelination, and synapse formation (Mei and Xiong, 2008). Interestingly, ErbB4 expression in the cortex is particularly abundant among PV+ fast-spiking interneurons (Fazzari et al., 2010; Neddens and Buonanno, 2010; Neddens et al., 2011; Yau et al., 2003), and functional studies have shown that it controls several aspects of their maturation and function (Fazzari et al., 2010; Shamir et al., 2012; Ting et al., 2011; Wen et al., 2010; Woo et al., 2007). As genetic variation in ERBB4 influences GABA levels in humans (Luykx et al., 2012; Marenco et al., 2011), these observations suggest a plausible link between abnormal ERBB4 signaling and GABAergic function in schizophrenia (Rico and Marín, 2011).

Here, we have analyzed the function of ErbB4 in the wiring of the two main classes of fast-spiking interneurons, chandelier

and basket cells. We find that specific loss of *Erbb4* from these interneurons during development causes cellular, physiological, and behavioral deficits that are highly reminiscent of phenotypes observed in schizophrenia. These results suggest that disruption of the function of fast-spiking interneurons might be a core feature of the disorder.

RESULTS

Generation of Conditional *Erbb4* Mutants

We generated conditional *Erbb4* mutant mice by breeding *Lhx6-Cre* mice with mice carrying loxP-flanked (F) *Erbb4* alleles (Golub et al., 2004). Lhx6 is a transcription factor expressed by postmitotic neurons derived from the medial ganglionic eminence (MGE), including most PV+ and somatostatin (SST+) cortical interneurons (Fogarty et al., 2007; Lavdas et al., 1999). Because ErbB4 is expressed in the cortex by most PV+ but few SST+ interneurons (Fazzari et al., 2010; Neddens and Buonanno, 2010; Yau et al., 2003), *Lhx6-Cre;Erbb4*$^{F/F}$ mice (conditional *Erbb4* mutants, for brevity) represent a rather selective model of *Erbb4* deletion in PV+ interneurons from early stages of corticogenesis (Figure S1A available online). Analysis of cortical lysates revealed a very prominent decrease of ErbB4 protein levels in conditional *Erbb4* mutants compared to controls (Figures S1B and S1C), and very few PV+ cortical interneurons continue to express ErbB4 in these mice (Figures S1D–S1F′). The remaining few PV+ interneurons that contain ErbB4 are likely generated in the preoptic area (Gelman et al., 2011), where *Lhx6* is not expressed (Flames et al., 2007).

We next examined the distribution of PV+ interneurons in the cortex of control and conditional *Erbb4* mutants. ErbB4 is required for the tangential migration of cortical interneurons (Flames et al., 2004), but postmitotic deletion of *Erbb4* does not result in the complete removal of ErbB4 protein before interneurons reach the cortex, due to the slow turnover of this receptor (Fazzari et al., 2010). Consistently, we observed no differences in the tangential migration of interneurons between controls and conditional *Erbb4* mutants (data not shown). In addition, the general organization and density of GABA cells and PV+ interneurons in different cortical regions was similar between both genotypes (Figures S1G–S1I). Thus, postmitotic removal of *Erbb4* from PV+ interneurons is not sufficient to impair their migration into the cerebral cortex. Consequently, *Lhx6-Cre;Erbb4*$^{F/F}$ mutants represent a suitable model to analyze the precise function of ErbB4 in the wiring of specific classes of PV+ interneurons.

Decreased Excitatory Synapses in PV+ Interneurons Lacking ErbB4

We have previously shown that PV+ interneurons receive less excitatory terminals in interneuron-specific *Erbb4* conditional mutants (Fazzari et al., 2010), a finding that is consistent with the idea that ErbB4 promotes the development of excitatory synapses onto interneurons in vitro (Ting et al., 2011). To elucidate whether different classes of PV+ interneurons are equally dependent on ErbB4 function, we independently analyzed the two main classes of fast-spiking interneurons by carrying out retroviral labeling experiments in which the cell-autonomous function of ErbB4 can be assessed in morphologically identified cortical interneurons. In brief, we used ultrasound imaging to focally inject low titer retroviruses encoding *Cre* and *Gfp* (*rv::Gfp-i-Cre*) into the MGE of control and conditional *Erbb4* mutant embryos at E13.5 (Figure 1A), when many PV+ interneurons are being generated (Rymar and Sadikot, 2007). Retroviral infection into the MGE results in the widespread labeling of isolated cortical interneurons at P30. We first analyzed the density of VGlut1+ terminals contacting chandelier cells (Figure 1B) and observed that the soma and dendrites of neocortical chandelier cells lacking *Erbb4* received significantly less VGlut1+ terminals than control cells (Figures 1C–1G and S2A–S2E). We next turned our attention to fast-spiking basket cells, identified by their characteristic morphology and immunoreactivity for PV (Figure 1H). We observed that the soma and dendrites of neocortical PV+ basket cells lacking ErbB4 received significantly fewer VGlut1+ terminals than control cells (Figures 1I–1M and S2F–S2I).

We next analyzed whether the loss of excitatory terminals was paralleled by corresponding changes in postsynaptic markers. We found that the reduction in the density of VGlut1+ terminals found in *Erbb4* mutant chandelier and PV+ basket cells compared to controls was matched by an equivalent reduction in the density of postsynaptic PSD95 clusters and VGlut1+/PSD95+ clusters (Figures S3A–S3L).

We then measured synaptic activity with whole-cell recordings from hippocampal PV+ fast-spiking interneurons in acute slices obtained from P20–P22 control and conditional *Erbb4* mutant mice (Figure 1N). Analysis of miniature excitatory postsynaptic currents (mEPSCs) showed a significant decrease in the frequency of synaptic events in PV+ interneurons in the stratum oriens of conditional *Erbb4* mutants compared to controls, with no changes in the amplitude of mEPSCs (Figures 1O–1Q). These observations are consistent with alterations in excitatory glutamatergic synapses and altogether, the data demonstrate that fast-spiking chandelier and basket cells require ErbB4 to receive a normal complement of excitatory glutamatergic synapses.

Heterogeneous Defects in Fast-Spiking Interneuron Synapses Lacking ErbB4

We next studied the consequences of deleting *Erbb4* in the formation of inhibitory synapses by specific classes of fast-spiking interneurons. We have previously shown that neocortical chandelier cells lacking ErbB4 make fewer synapses than normal (Fazzari et al., 2010). Because these results have been challenged by recent work (Neddens et al., 2011), we carried out new experiments to analyze the density of synaptic boutons present in candlestick arrays made by chandelier cells identified through retroviral labeling of MGE progenitors. We observed a significant loss of presynaptic boutons in chandelier cells lacking ErbB4 compared to control cells (Figures 2A–2E).

To corroborate this observation, we analyzed the postsynaptic component of axo-axonic synapses in conditional *Erbb4* mutants. We quantified $\alpha 2$ subunit of the $GABA_A$ receptor ($GABA_A\alpha 2$) clusters, because this subunit is enriched at axo-axonic synapses in the axon initial segment (AIS) (Loup et al., 1998; Nusser et al., 1996). We found that the AIS of hippocampal pyramidal cells contained significantly fewer $GABA_A\alpha 2$ clusters in conditional *Erbb4* mutants than in controls (Figures 2F–2I). A similar deficit was observed in the lateral entorhinal cortex

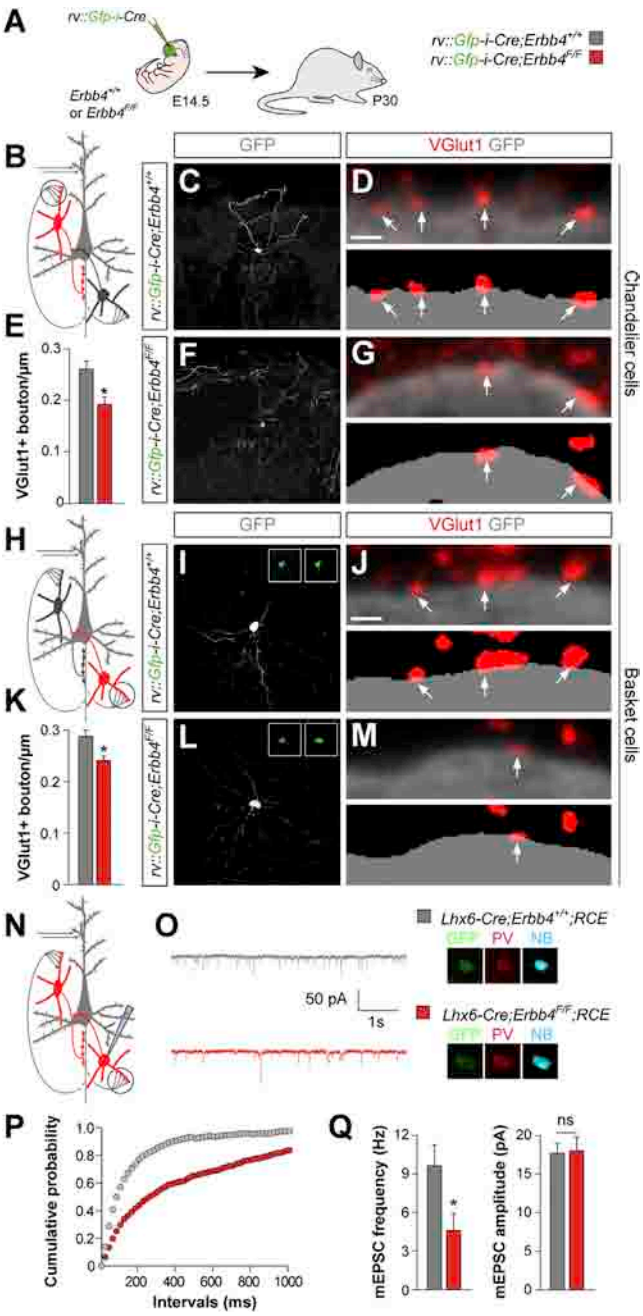

Figure 1. Chandelier and Basket Cells Require ErbB4 to Receive Normal Numbers of Excitatory Inputs

(A) Experimental design.

(B) Scheme of ErbB4 chandelier cell-specific deletions (red cell). The circle indicates the synapses analyzed in this experiment.

(C and D) Control chandelier cells. VGlut1+ boutons (arrows) apposed to the soma (D). Scale bar represents 1 μm.

(E) Density of VGlut1+ boutons contacting the soma of chandelier cells. Binary images used for quantification (bottom panels in D and G). *p < 0.05, t test; n = 9 control and 7 mutant cells, three brains per genotype.

(F and G) *Erbb4* mutant chandelier cells. VGlut1+ boutons (arrows) apposed to the soma (G). Scale bar represents 1 μm.

(H) Scheme of ErbB4 basket cell-specific deletions (red cell). The circle indicates the synapses analyzed in this experiment.

(I and J) Control PV+ basket cells. VGlut1+ boutons (arrows) apposed to the soma (J).

(K) Density of VGlut1+ boutons contacting the soma of PV+ basket cells. Binary images used for quantification (bottom panels in J and M). $p < 0.05$, t test; n = 9 control and 8 mutant PV+ basket cells, three brains per genotype.

(L and M) *Erbb4* mutant PV+ basket cells. VGlut1+ boutons (arrows) apposed to the soma (M).

(N) Scheme of recordings (pipette) performed in hippocampal interneurons.

(O) Traces of mEPSCs in GFP+ (green), PV+ (red), neurobiotin-filled (blue) control and mutant interneurons.

(P) Cumulative probability plot.

(Q) mEPSC frequencies, *p < 0.05 and amplitudes, p = 0.9, t test. n = 10 cells, from five controls and n = 10 cells from four mutants.

See also Figures S1, S2 and, S3.

(Figure 2I). The length of candlesticks visualized with the presynaptic marker GABA transporter-1 (GAT-1) in the lateral entorhinal cortex was also reduced in the absence of ErbB4 (data not shown). Altogether, these results demonstrate that ErbB4 is necessary for the development and/or maintenance of axo-axonic synapses in the cortex.

We next examined whether ErbB4 function was also required for the formation of somatic inhibitory synapses by PV+ basket cells. We quantified the number of PV+ boutons contacting the soma of NeuN+ pyramidal cells in the CA1 region of control and conditional *Erbb4* mutants (Figure 2J). The number of PV+ terminals surrounding the soma of hippocampal neurons was similar between control and conditional *Erbb4* mutants (Figures 2K–2M). There were no differences in the density of postsynaptic Gephyrin+ clusters and PV+/ Gephyrin+ clusters in the soma of pyramidal cells of conditional *Erbb4* mutants and control mice (Figures S4A–S4G). Likewise, the size of the somatic PV+ terminals was also indistinguishable between both genotypes (Figures 2K–2M), suggesting that ErbB4 function is dispensable for PV+ basket cell synapses.

We also analyzed the organization of the postsynaptic compartment in the basket cell. We quantified the density of clusters of the α1 subunit of the $GABA_A$ receptor ($GABA_A\alpha1$) present in the ring-like PV+ structures that identify the inhibitory perisomatic synapses contacting pyramidal cells (Chattopadhyaya et al., 2007; Huang et al., 1999). We observed a small but significant decrease in the number of $GABA_A\alpha1$+ clusters found in the soma of pyramidal cells in conditional *Erbb4* mutants compared to controls (Figures 2N–2R). The fraction of PV+ terminals contacting a postsynaptic $GABA_A\alpha1$+ cluster and the number of PV+/$GABA_A\alpha1$+ clusters in the soma of pyramidal cells was also significantly reduced, whereas no differences were observed in the density of somatic $GABA_A\alpha1$+ clusters outside PV+ terminals (Figures 2N–2R).

We next measured synaptic activity with whole-cell recordings from hippocampal CA1 pyramidal neurons in acute slices obtained from P20–P22 control and conditional *Erbb4* mutant mice (Figure S4H). Analysis of miniature inhibitory postsynaptic currents (mIPSCs) showed a significant decrease in the frequency of synaptic events in *Erbb4* mutants compared to controls, whereas the amplitude of mIPSCs remained unchanged (Figures S4I–S4K). The reduction in the frequency of mIPSCs could be caused by a decrease in the number of release sites, a decrease in the probability of GABA release, or both. To

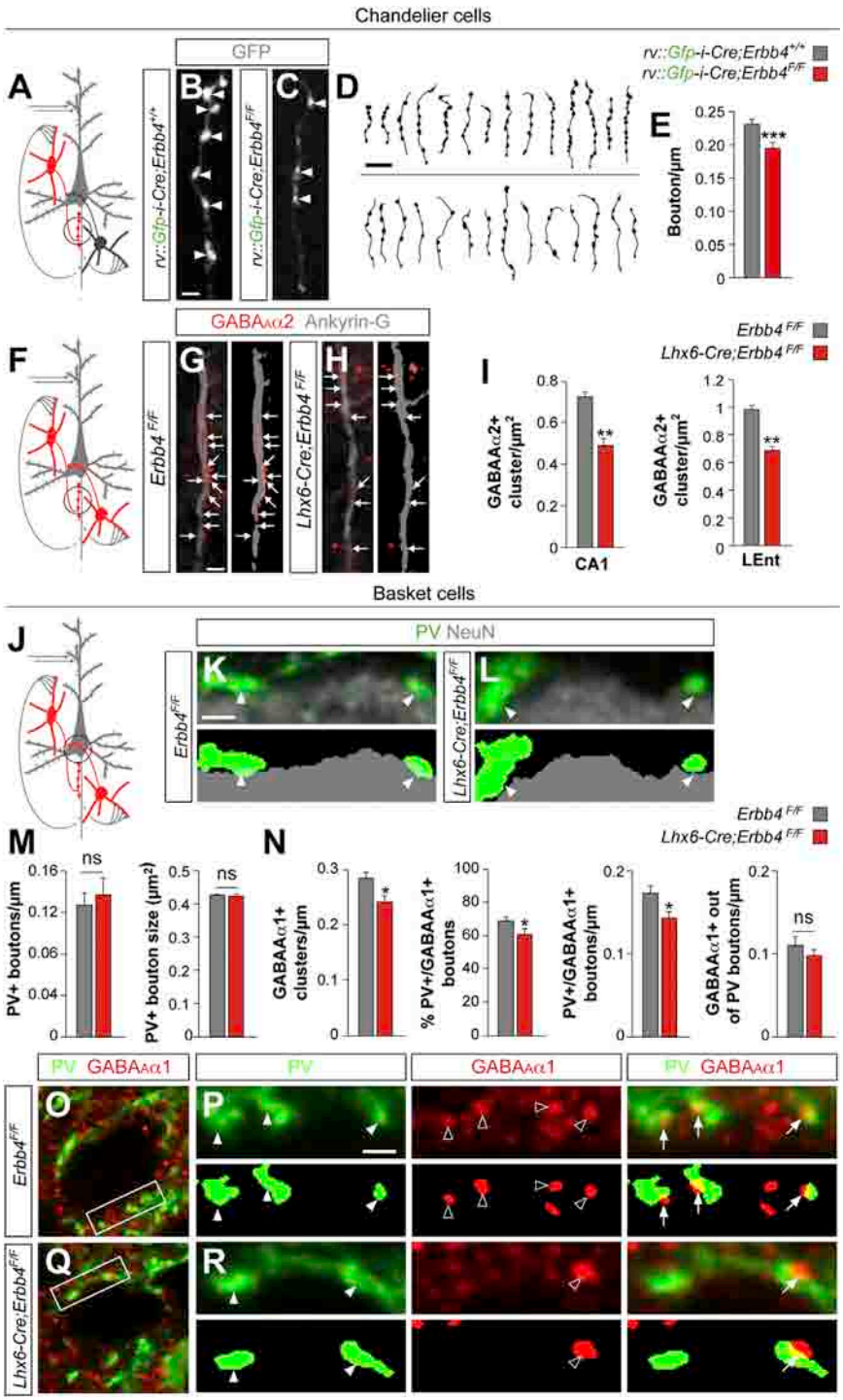

Figure 2. Deletion of ErbB4 Differentially Affects Chandelier and Basket Cells Synapses

(A) Scheme of ErbB4 chandelier cell-specific deletion.

(B and C) Candlesticks from control and mutant chandelier cells with synaptic boutons (arrowheads). Scale bars represent 2 µm.

(D) Candlestick drawings from control (up) and mutant (down). Scale bar represents 10 µm.

(E) Density of boutons in candlesticks. ***p < 0.001, t test; n = 12 control and 8 mutant cells, three brains per genotype.

(F) Scheme of ErbB4 deletion in fast-spiking interneurons.

(G and H) $GABA_A\alpha2$+ receptor clusters (arrows) within Ankyrin-G+ AIS of hippocampal pyramidal cells in control and mutant mice. Scale bars represent 2 µm.

(I) Density of $GABA_A\alpha2$+ clusters in CA1 and lateral entorhinal cortex (LEnt). **p < 0.01, t test; n = 30 AIS, three brains per genotype.

(J) Scheme of ErbB4 deletion in CA1 fast-spiking interneurons.

(K and L) PV+ boutons apposed to NeuN+ pyramidal cell somas in control and mutant mice. Scale bars represent 1 µm.

(M) Density and size of PV+ boutons; n = 75 cells, three brains per genotype. ns, no significant differences.

(N) Density of $GABA_A\alpha1$+ clusters per PV+ bouton ring, percentage of PV+ boutons containing $GABA_A\alpha1$+ clusters, density of PV+ terminals containing $GABA_A\alpha1$+ clusters, and density of $GABA_A\alpha1$+ clusters outside PV+ terminals. *p < 0.05; t test; n = 125 cells, six brains per genotype. ns, no significant differences.

(O–R) Ring-like structure with PV+ boutons and $GABA_A\alpha1$+ clusters in control and mutant mice. (P) and (R) are high-magnification images of (O) and (Q), respectively. PV+ boutons (full arrowheads), $GABA_A\alpha1$+ clusters (open arrowheads) and colocalization (arrows). Scale bars represent 1 µm.

See also Figures S1 and S4.

distinguish between these possibilities, we analyzed pair-pulse ratios in control and conditional *Erbb4* mutants and found no differences between both experimental groups (Figure S4L), which indicated that the probability of release does not change in the absence of ErbB4. These results confirmed that pyramidal cells receive a reduced number of inhibitory synapses in conditional mutants in which *Erbb4* has been deleted from fast-spiking interneurons. Based on our morphological analyses, these deficits are primarily due to defects in chandelier cell synapses.

Additional Cellular Schizophrenia-like Deficits in Conditional *Erbb4* Mutants

To explore whether loss of ErbB4 in PV+ interneurons could lead to additional GABAergic defects, we analyzed the expression of the two isoforms of GAD that are responsible for the synthesis of GABA, GAD65, and GAD67, in control and conditional *Erbb4* mutants (Figure 3A). We found that GAD67 protein levels are reduced in the cortex of conditional *Erbb4* mutants compared to controls, whereas GAD65 remains unchanged (Figures 3B and 3C). Total PV protein levels were also reduced in conditional *Erbb4* mutants compared to controls (Figures 3B

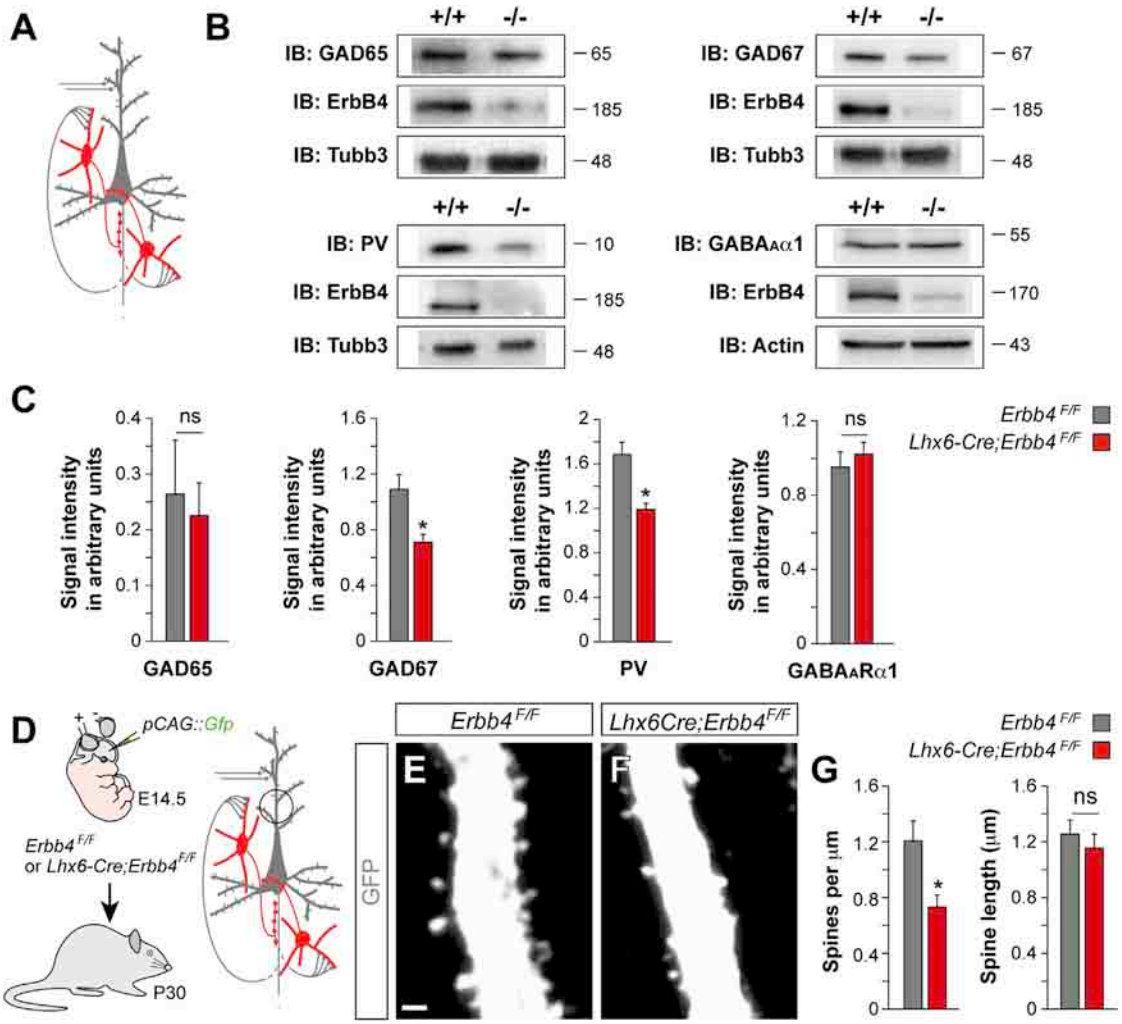

Figure 3. Additional Cellular Deficits in *Erbb4* Conditional Mutants

(A) Scheme of ErbB4 deletion in fast-spiking interneurons.

(B and C) Immunoblots and quantification of GAD65, GAD67, PV, and $GABA_A\alpha1$ proteins from hippocampus and somatosensory cortex (SSCx) homogenates in control and mutant mice. *$p < 0.05$; ns, no significant differences, t test; $n = 4$.

(D) Experimental design and scheme of ErbB4 deletion in fast-spiking interneurons.

(E and F) Hippocampal GFP+ pyramidal cell dendrites and spines in control and mutant mice. Scale bar represents 1 µm.

(G) Density and length of spines. *$p < 0.05$; t test; $n = 10$ dendrites, three brains per genotype.

See also Figure S1.

and 3C). In contrast, no differences were observed in total $GABA_A\alpha1$ protein levels between both genotypes (Figures 3B and 3C).

We also quantified the number of dendritic spines in hippocampal CA1 pyramidal cells labeled with GFP (Figure 3D) and found a significant decrease in the number of dendritic spines in conditional *Erbb4* mutants compared to controls, whereas no changes in the length of the spines was observed (Figures 3E–3G). The reduction in the number of spines seemed confined to the proximal aspect of the apical dendrite, because no major differences were observed in the number of spines located in distal dendrites (data not shown). These results demonstrate that pyramidal cell deficits may arise secondary to the loss of ErbB4 in specific classes of interneurons.

Enhanced Excitatory and Inhibitory Activities in Conditional *Erbb4* Mutants In Vitro

We next studied to what extent hippocampal network activity was affected by the loss of synapses observed in *Erbb4* conditional mutants. In particular, we reasoned that the loss of excitatory synapses onto both classes of fast-spiking interneurons, together with the reduction in the number of inhibitory synapses made by chandelier cells, should cause an overall reduction of inhibition on pyramidal cells and these neurons should be more active in the cortex of *Erbb4* conditional mutants. To test this hypothesis, we recorded spontaneous excitatory currents (sEPSCs) in CA1 hippocampal pyramidal cells using whole cell patch-clamp in acute slices preparations from P20–P22 mice (Figure 4A). We observed that pyramidal cells received more

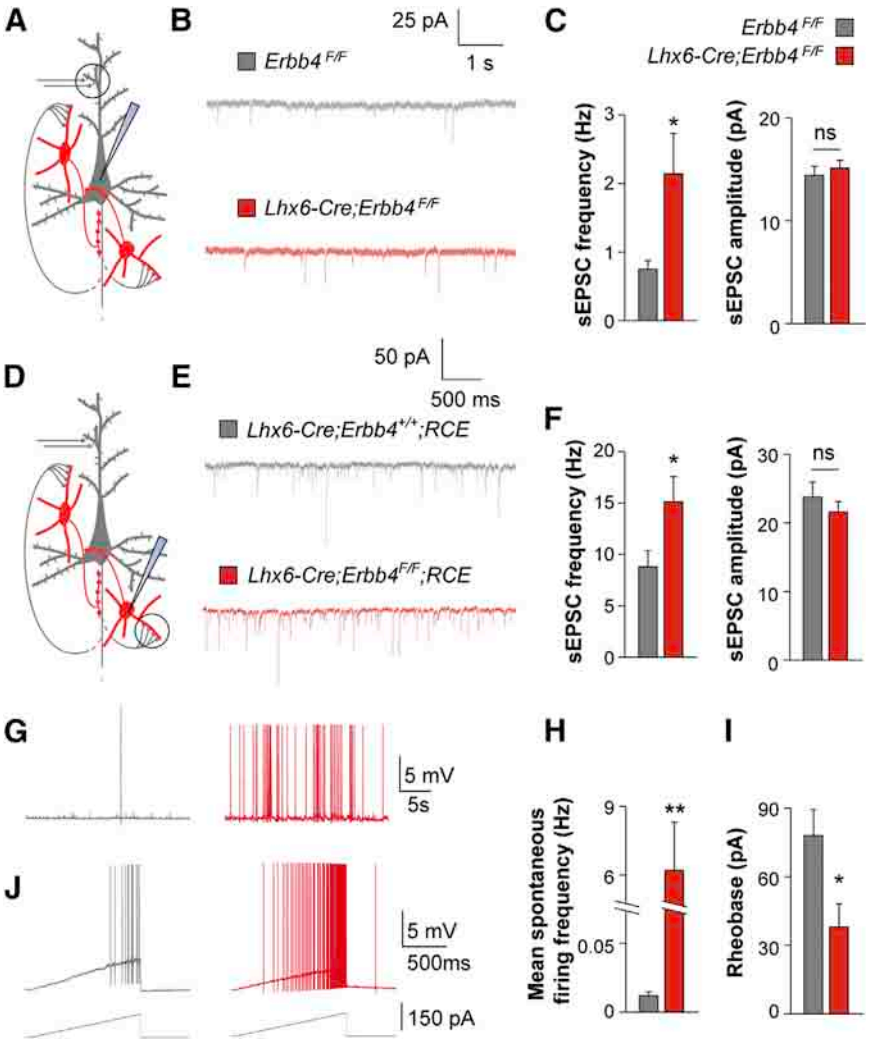

Figure 4. Enhanced Excitatory and Inhibitory Activities in Conditional *Erbb4* Mutants In Vitro

(A) Scheme of ErbB4 deletion in fast-spiking interneurons and recording location (pipette) in the hippocampus.

(B) Traces of sEPSCs in control and mutant mice.

(C) sEPSCs frequencies (*$p < 0.05$) and amplitudes ($p = 0.5$), t test. n = 15 and 16 neurons from five controls and four mutant mice, respectively.

(D) Scheme of ErbB4 deletion in fast-spiking interneurons and recording location (pipette) in the hippocampus.

(E) Traces of sEPSCs in control and mutant mice.

(F) sEPSCs frequencies (*$p < 0.05$) and amplitudes ($p = 0.4$), t test. n = 12 and 12 neurons from eight controls and five mutant mice, respectively.

(G) Traces of spontaneous firing of PV+ fast-spiking interneurons from control and mutant mice, recorded at resting membrane potential (Vrest = −60 mV and −62 mV, respectively).

(H and I) Mean spontaneous firing frequency (H) and Rheobase (I), **$p < 0.01$, *$p < 0.05$, t test. n = 10 and 11 neurons from four controls and five mutant animals, respectively.

(J) Traces of spontaneous firing of PV+ fast-spiking interneurons from control and mutant mice, recorded after ramp stimulation.

See also Figure S1 and Table S1.

excitatory drive in conditional *Erbb4* mutants than in controls, as revealed by a significant increase in sEPSCs frequencies (Figures 4B and 4C). In contrast, we found no changes in the amplitude of these currents between control and mutant pyramidal cells (Figures 4B and 4C).

We next wondered whether the increased activity observed in pyramidal cells of *Erbb4* mutants could also enhance their excitatory drive onto fast-spiking interneurons. To this end, we recorded sEPSCs from PV+ fast-spiking interneurons (Figure 4D) and observed a significant increase in sEPSC frequencies in *Erbb4* mutant interneurons compared to control cells, with no changes in their amplitude (Figures 4E and 4F). Interestingly, we found a significant increase in the NMDA/AMPA ratio of these currents (control: 0.26 ± 0.05; *Erbb4* mutant: 0.66 ± 0.14; n = 8 neurons per genotype from three mice in each case; $p < 0.05$, t test), which was caused by a significant reduction in the amplitude of AMPA currents in *Erbb4* mutant interneurons (control: 257 ± 87 pA; *Erbb4* mutant: 69 ± 12 pA; $p < 0.05$, t test). Because we did not observe any difference in the amplitude of mEPSCs recorded from fast-spiking interneurons (Figure 1Q), these results suggested that the excitatory synapses that are lost from PV+ interneurons in *Erbb4* mutants are preferentially enriched in AMPA receptors.

To examine the activity of PV+ fast-spiking interneurons, we performed current-clamp recordings and found no significant alterations in the basic membrane properties of the PV+ fast-spiking interneurons in *Erbb4* mutants compared to control mice in response to 500 ms depolarizing steps (Table S1). However, we observed that most PV+ interneurons displayed a delay to the first spike at threshold potential for spikes in *Erbb4* mutants (n = 9/10 cells) compared to controls (n = 5/11 cells). Most PV+ interneurons also spontaneously fired at resting membrane potential in both controls (n = 7/11 cells) and *Erbb4* mutants (n = 9/10 cells). However, we found that the mean spontaneous firing frequency of PV+ fast-spiking interneurons is largely increased in the absence of ErbB4 (Figures 4G and 4H). Moreover, application of 5 s depolarizing ramps revealed a lower rheobase in the *Erbb4* mutant PV+ interneurons than controls (Figures 4I and 4J) without changes in the threshold potential for spikes (*Lhx6-Cre;Erbb4*$^{+/+}$*;RCE* controls, −42.9 ± 3.6 mV; *Lhx6-Cre;Erbb4*$^{F/F}$*;RCE* mutants, −48.1 ± 3.0 mV; $p = 0.3$, t test). This enhanced excitability leads to a significant increase in the number of action potentials elicited during the ramp by the PV+ fast-spiking interneurons (*Lhx6-Cre;Erbb4*$^{+/+}$*;RCE* controls, 23 ± 8; *Lhx6-Cre;Erbb4*$^{F/F}$*;RCE* mutants, 102 ± 26; $p < 0.05$, t test). Altogether, these results suggested that the loss of specific synapses in *Erbb4* mutants leads to a concomitant enhancement in the activity of both pyramidal cells and fast-spiking interneurons.

Enhanced Excitability and Hypersynchrony in Conditional *Erbb4* Mutants In Vivo

To identify the potential consequences of these network alterations in vivo, we carried out local field potential (LFP) recordings in the hippocampus of urethane-anesthetized control and conditional *Erbb4* mutant mice. We acutely implanted 32-channel silicon probe arrays in the dorsal hippocampus of anesthetized mice, which allowed the simultaneous recording of LFPs through the dentate gyrus (DG) and the CA1 area of the hippocampus (Figure 5A). Compared to controls, conditional *Erbb4* mutants exhibited a marked increased in oscillatory power in the resting-state (Figures 5B and 5C). Frequent bursts of high-frequency oscillations were observed in the DG, which often correlated with simultaneous increases in oscillatory power in the CA1 region and, occasionally, the overlying neocortex (Figures 5B and 5C). Consistently, DG-CA1 coherence increased significantly in conditional *Erbb4* mutants, especially at relatively high frequencies (Figure 5D). Closer inspection of these resting-state recordings revealed the presence of spontaneous and fully developed field population spikes in the DG closely resembling field potentials evoked by perforant path stimulation (Figure 5E). This finding strongly suggests the presence of synchronous activity bursts already in the entorhinal cortex, a region in which we also found deficits of interneuron synapses in conditional *Erbb4* mutant mice (Figure 2I). To further investigate neuronal synchrony in the hippocampus, we measured the input-output function in the trisynaptic circuit (DG → CA3 → CA1) by correlating the excitatory postsynaptic potential (EPSP) in the DG in response to perforant path stimulation (~2 ms delay) and the population spikes recorded in CA1 (~8 ms delay). We observed that the polysynaptic propagation of activity in the hippocampal formation is largely facilitated in conditional *Erbb4* mutant mice (Figures 5E, arrows, and 5F).

These observations were replicated in ketamine-anesthetized conditional *Erbb4* mutant mice (Figures S5A–S5E), which revealed that the enhanced oscillatory power observed in mice lacking ErbB4 was not directly related to a particular anesthetic compound. In some cases, however, we observed that ketamine led to epileptic hypersynchrony in conditional *Erbb4* mutants (n = 3 out of six mice, data not shown), a phenomenon that was never observed in ketamine-anesthetized controls or in urethane-anesthetized control or *Erbb4* mutant mice. As ketamine is an N-methyl-D-aspartate (NMDA) receptor antagonist, these results suggested that NMDA receptor blockage enhances the physiological disturbances caused by the loss of ErbB4 in fast-spiking interneurons.

We observed a sustained elevation in relative power for all frequencies above 4 Hz in the CA1 area of conditional *Erbb4* mutants compared to controls (Figure 5G). This increase was significant for the theta, alpha, beta, and gamma bands (Figures 5H) and was particularly perceptible with wavelet analyses (Figures 5I and 5J). The dramatic alteration of hippocampal rhythms was also evident in the CA1 area of ketamine-anesthetized *Erbb4* mutants (Figures S5F–S5I) and in the DG independently of the anesthetic compound used in the experiments (Figure S6). Altogether, these experiments suggested that the relatively subtle perturbation in the connectivity of fast-spiking interneurons caused by the loss of ErbB4 has a major impact in the generation of hippocampal rhythms.

Impaired Hippocampal-Prefrontal Synchrony in Conditional *Erbb4* Mutants

We examined whether loss of ErbB4 would also affect baseline rhythms in the neocortex. To this end, we recorded spontaneous LFPs in the prefrontal cortex of control and conditional *Erbb4* mutant mice (Figure 6A). Field recordings during urethane anesthesia revealed more subtle differences in resting-state oscillations between both genotypes than in the hippocampus (Figures 6B and 6C). In particular, a net increase in the relative power of the gamma band was observed in the infralimbic cortex of conditional *Erbb4* mutants compared to control mice (Figure 6D). These differences were also observed in ketamine-anesthetized mice (Figure S7).

We then tested whether synchrony between the hippocampus and the prefrontal cortex was affected in conditional *Erbb4* mutants by analyzing the cross-correlation between simultaneous electrophysiological recordings in CA1 and the infralimbic (IL) and prelimbic (PrL) cortices in resting conditions. We observed a significant reduction in synchrony between the hippocampus and both subdivisions of the prefrontal cortex of conditional *Erbb4* mutants compared to controls, whereas cross-correlation coefficients between IL and PrL did not vary (Figure 6E). Consistently, hippocampal-prefrontal coherence in the theta rhythm was prominently diminished in conditional *Erbb4* mutants compared to control mice (Figure 6F). These findings suggested that ErbB4 function is required for normal baseline rhythms within local cortical networks and that loss of ErbB4 in fast-spiking interneurons disrupts the long-range synchrony between the hippocampus and prefrontal cortex in resting-state conditions.

Increased Gamma Oscillations in the Hippocampus of Freely Moving Conditional *Erbb4* Mutants

To examine hippocampal rhythms in a more physiological context, we performed recordings in freely moving control and conditional *Erbb4* mutant mice. To this end, we implanted tetrodes in the hippocampal pyramidal cell layer and recorded electrophysiological activity in mice exploring a square open field. We analyzed epochs of activity in which speed of movement was above 5 cm/s to reduce variability in LFP recordings, and we verified that the mean speed of the epochs analyzed was similar for both genotypes (controls, V = 9 ± 0.4 cm/s; *Erbb4* mutants, V = 10 ± 0.2 cm/s; p = 0.63, t test).

Analysis of spontaneous LFPs in the pyramidal layer of hippocampal CA1 in conditional *Erbb4* mutants revealed a marked increase in activity compared to controls (Figures 7A–7D). In addition, we observed spontaneous hypersynchronic events in *Erbb4* mutants that we never observed in control mice (Figures 7A and 7B). These events were qualitatively similar to the spontaneous population spikes observed in the hippocampus of *Erbb4* mutants under anesthesia (Figures 5E and S5E).

We next analyzed the relative power of oscillations in control and conditional *Erbb4* mutant mice. We also observed an increase in the relative power of gamma oscillations in *Erbb4* mutants compared to control mice (Figures 7E–7H). Finally, we

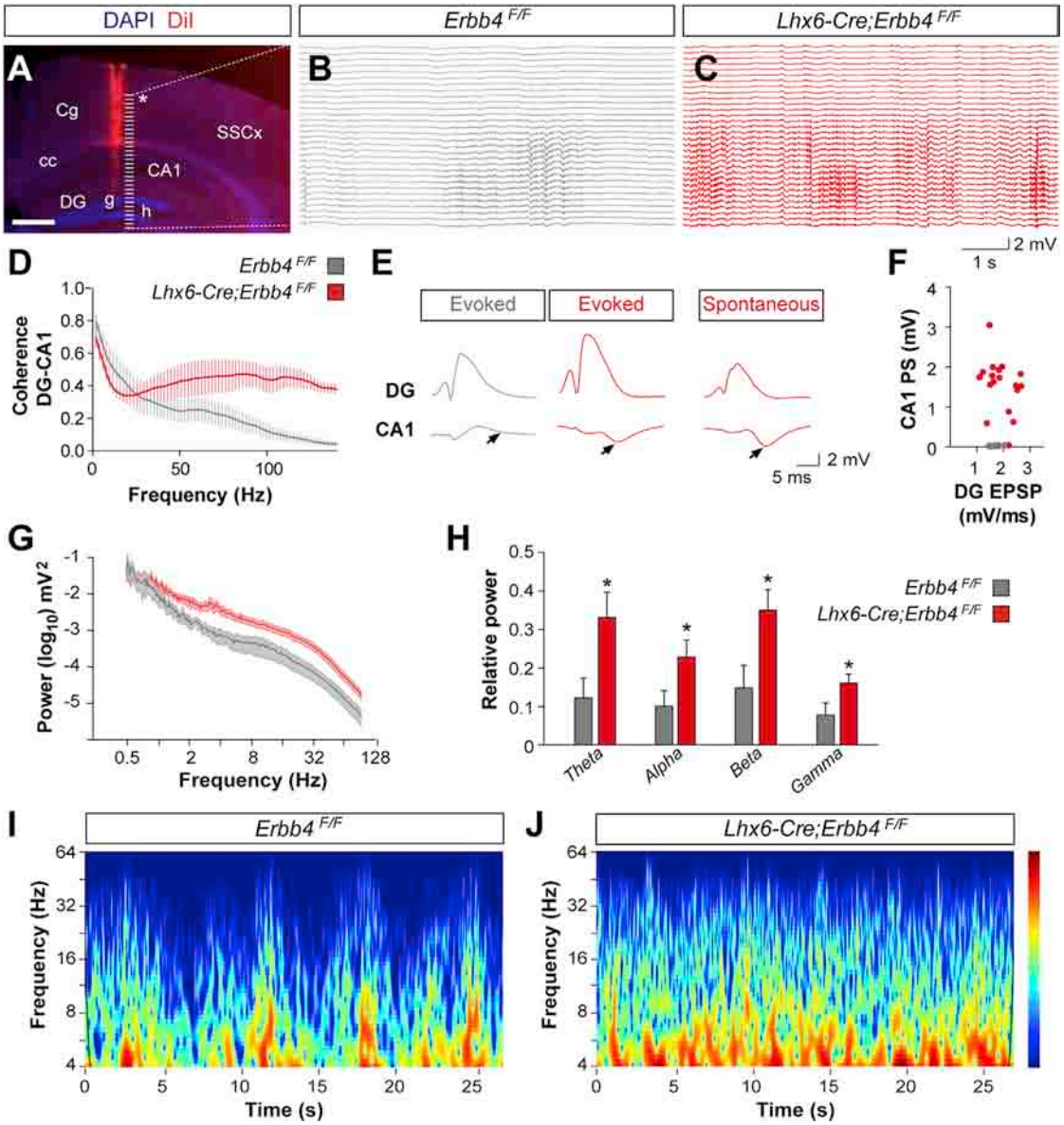

Figure 5. Increased Activity and Oscillations in the Hippocampus of Urethane-Anesthetized *Erbb4* Conditional Mutants

(A) Dye trace (red) indicates the probe implantation site. CA1 region of the hippocampus cc, corpus callosum; Cg, cingulated cortex; DG, dentate gyrus; g, granular cell layer; h, hilus; SSCx, somatosensory cortex. Scale bar represents 500 μm.

(B and C) Traces of spontaneous LFP of control (B) and mutant (C) mice.

(D) Coherence between DG and CA1 region of the hippocampus in control (n = 4) and mutant (n = 6) mice.

(E) Evoked and spontaneous LFP in control and mutant mice. Arrows point to the tri-synaptic EPSP in CA1.

(F) Input-output curves in the tri-synaptic hippocampal circuit. EPSPs recorded in the molecular layer upon perforant stimulation are plotted against the trisynaptically evoked PS in the CA1. ***p < 0.001, t test with Welch's correction when appropriate; n = 3 controls and 4 mutant mice.

(G) Power spectrum of CA1 LFP from 0.5–128 Hz in control (n = 4) and mutant (n = 6) mice.

(H) CA1 relative LFP band-power in the theta (4–8 Hz), alpha (8–13 Hz), beta (13–30 Hz), and gamma (30–125 Hz) frequency bands *p < 0.05, t test; n = 4 control and 6 mutant mice.

(I and J) Wavelet spectra of CA1 LFP from control (I) and mutant (J) mice. Color scale, 0–8.4 mV^2.

See also Figures S1, S5, and S6.

examined whether the modulation of gamma oscillations by the theta cycle was altered in conditional *Erbb4* mutants. We estimated the center of mass for the gamma power distribution and calculated its relationship to the theta phase (Figures 7I and 7J). We found that the power of gamma oscillations mean center of mass was slightly displaced in the theta cycles of the *Erbb4* mutant compared to controls (mean phase: controls, 200.12 ± 0.61°; *Erbb4* mutants, 196.14 ± 0.66°; n = 4,

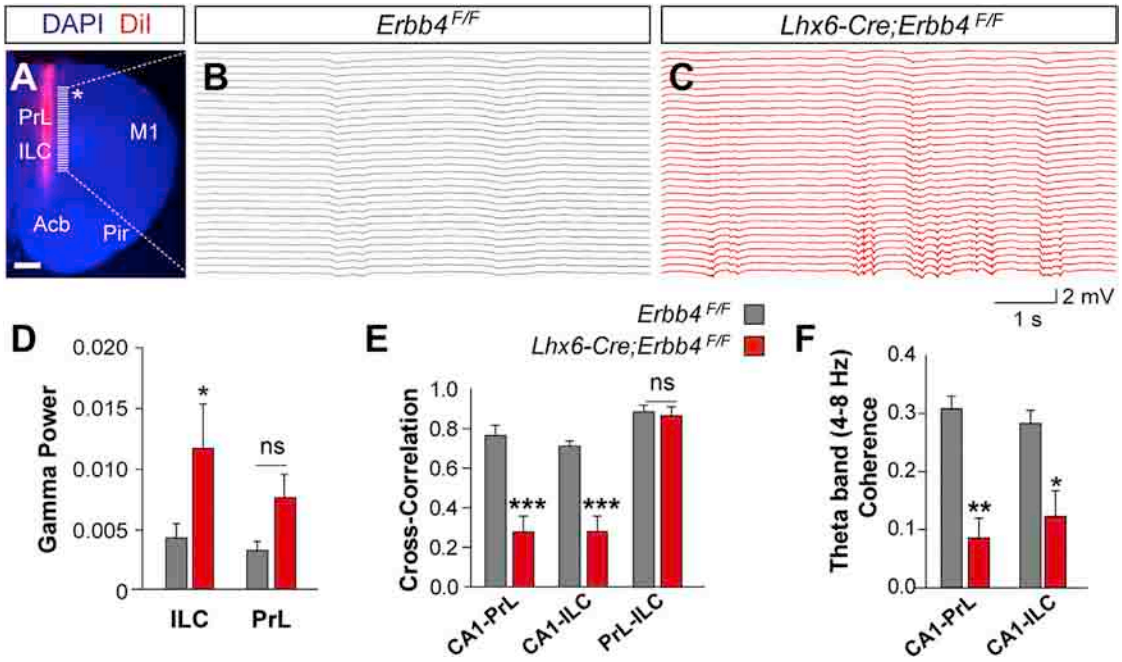

Figure 6. Impaired Synchrony between Hippocampus and Prefrontal Cortex in Urethane-Anesthetized *Erbb4* Conditional Mutants

(A) Dye trace (red) indicates the probe implantation site. Acb, accumbens; ILC, infralimbic cortex; M1, primary motor cortex; Pir, piriform cortex; PrL, prelimbic cortex. Scale bar represents 500 μm.

(B and C) Spontaneous LFPs traces from control and mutant mice.

(D) Relative LFP power in gamma frequency band (30–100 Hz) in prefrontal cortices. *$p < 0.05$: ns, no significant differences; t test with Welch's correction; n = 4 control and 6 mutant mice.

(E) Cross-correlation between CA1, IL, and PrL LFPs in control and mutant mice; ***$p < 0.001$; ns, no significant differences; two-way repeated-measures ANOVA with Bonferroni test as post hoc; n = 4 control and 6 mutant mice.

(F) Theta band critical coherence between hippocampus and prefrontal cortices in control and *Lhx6-Cre; Erbb4*$^{F/F}$ mutant mice; **$p < 0.01$, *$p < 0.05$; Mann-Whitney U test (p values corrected with Bonferroni); n = 4 control and 6 mutant mice.

See also Figures S1 and S7.

$p < 0.001$, Watson-Williams test). These experiments confirm a prominent increase in baseline gamma oscillations in the hippocampus of conditional *Erbb4* mutant mice.

Behavioral Deficits in Conditional *Erbb4* Mutants

To evaluate the functional consequences of the reported defects, we carried out behavioral analyses and found that conditional *Erbb4* mutant mice display a pronounced increase in locomotor activity (Figures 8A–8C), independently of the spatial dimensions, cognitive demand, or anxiety levels of the experiment. We next examined the emotional behavior of conditional *Erbb4* mutant mice using the elevated plus maze. We observed that both genotypes spent similar time in the central area of the apparatus (Figure 8D). However, conditional *Erbb4* mutants stayed significantly longer in the open (unprotected) arms than control mice (Figure 8D), which suggested reduced levels of anxiety in an aversive environment. We confirmed this finding with the marble-burying test and found that conditional *Erbb4* mutants buried significantly less marbles than controls and had shorter grooming episodes (Figure 8E).

We assessed sociability and preference for social interaction with the three-chambered social test. In this test, mouse exploratory behavior is scored through four sessions: habituation (empty cylinders), social familiar (familiar subject and empty cylinder), social stranger (stranger subject and empty cylinder), and preference for social novelty (familiar and stranger subjects). We observed a significant main effect of session and a significant interaction between session and genotype (repeated-measures ANOVA, $p < 0.001$ and $p < 0.05$, respectively; n = 15), which revealed an aberrant social behavior in conditional *Erbb4* mutants, as illustrated by the reduced sniffing preference for a familiar conspecific compared to the empty chamber, and increased sniffing in the chamber containing the empty cylinder (Figure 8F). These observations suggested impaired sociability in conditional *Erbb4* mutants. In addition, conditional *Erbb4* mutants displayed greater disregard for the familiar subject than controls in the preference for social novelty phase (Figure 8F). This behavior indicated impaired sociability toward familiar subjects, rather than altered social novelty preference. These differences could not be attributed to hyperactivity or lack of motivation, because the total time of exploration across sessions was similar between genotypes (Figure S8A).

We also examined nesting behavior in conditional *Erbb4* mutants to assess their ability to establish an organized behavior. Compared to controls, conditional *Erbb4* mutants were not able to form an identifiable nest within 24 hr and had

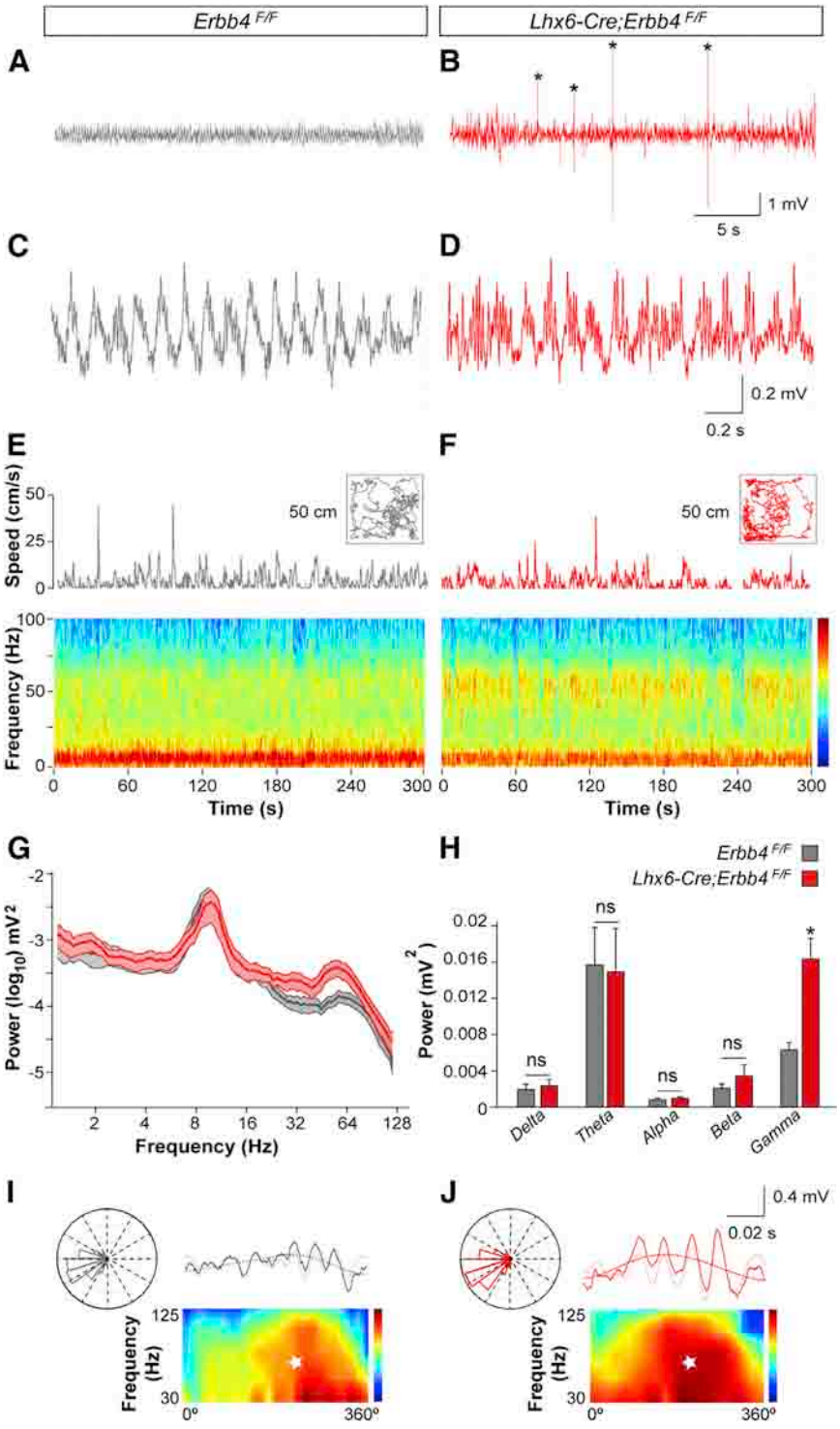

Figure 7. Increased Gamma Oscillations in the Hippocampus of Freely-Moving *Erbb4* Conditional Mutants

(A and B) Spontaneous LFPs from control (A) and mutant (B) mice. *ErbB4* mutants show hypersynchronic activity illustrated by the presence of spontaneous spike forms (asterisks).

(C and D) Higher magnification of (A) and (B).

(E and F) Tracks of control (E) and mutant (F) mice during spontaneous exploration in an open field (50 × 50 cm). Instantaneous speed of control (E) and mutant (F) mice for the depicted open fields and bottom spectrograms.

(G) Power spectrum of CA1 LFP from 0.5–100 Hz in control (n = 4) and mutant (n = 4) mice. Color scale, 75–110 Db.

(H) CA1 LFP band-power in the delta (0.5–3 Hz), theta (4–12 Hz), alpha (13–15 Hz), beta (16–30 Hz), and gamma (31–100 Hz) frequency bands *p < 0.05, t test; n = 4 control and 4 mutant mice.

(I and J) LFP together with filtered theta and gamma bands in control and mutant mice. Polar plot histograms and spectrograms with the center of mass for the gamma band (white star) for each theta cycle (degrees). Color scale, 75–95 Db.

See also Figure S1.

a tendency to scatter nesting material (Figures 8G and S8B). These results indicated an inability to properly nest building, a feature associated with poor planning of organized behavior and social withdrawal.

To test cortical cognitive function in conditional *Erbb4* mutants, we used the Y maze spontaneous alternation test. Even taking into account their hyperactivity pattern (Figure 8C), conditional *Erbb4* mutants displayed a significant reduction in alternation compared to control mice (Figure 8H), indicative of working memory dysfunction. Finally, we also analyzed sensorimotor gating using the prepulse inhibition (PPI) of the startle reflex paradigm. We observed impaired PPI in conditional *Erbb4* mutants compared to controls, although both genotypes have similar startle response amplitudes (Figure 8I).

DISCUSSION

Developmental loss of the neuregulin receptor ErbB4 from fast-spiking basket and chandelier cells causes synaptic defects in these neuronal populations and a profound functional reorganization of cortical networks. These alterations boost cortical oscillations, in particular in the gamma range, impair hippocampal-prefrontal theta synchrony, and disrupt emotional and social behaviors and cognitive function (Figure 9). Intriguingly, many of the abnormalities recapitulate salient pathophysiological features of schizophrenia (Lewis and Sweet, 2009; Lisman et al., 2008; Uhlhaas and Singer, 2012). Although genetic variation in the neuregulin/ErbB4 signaling pathway is only responsible for a small fraction of the genetic risk of schizophrenia (Harrison and Law,

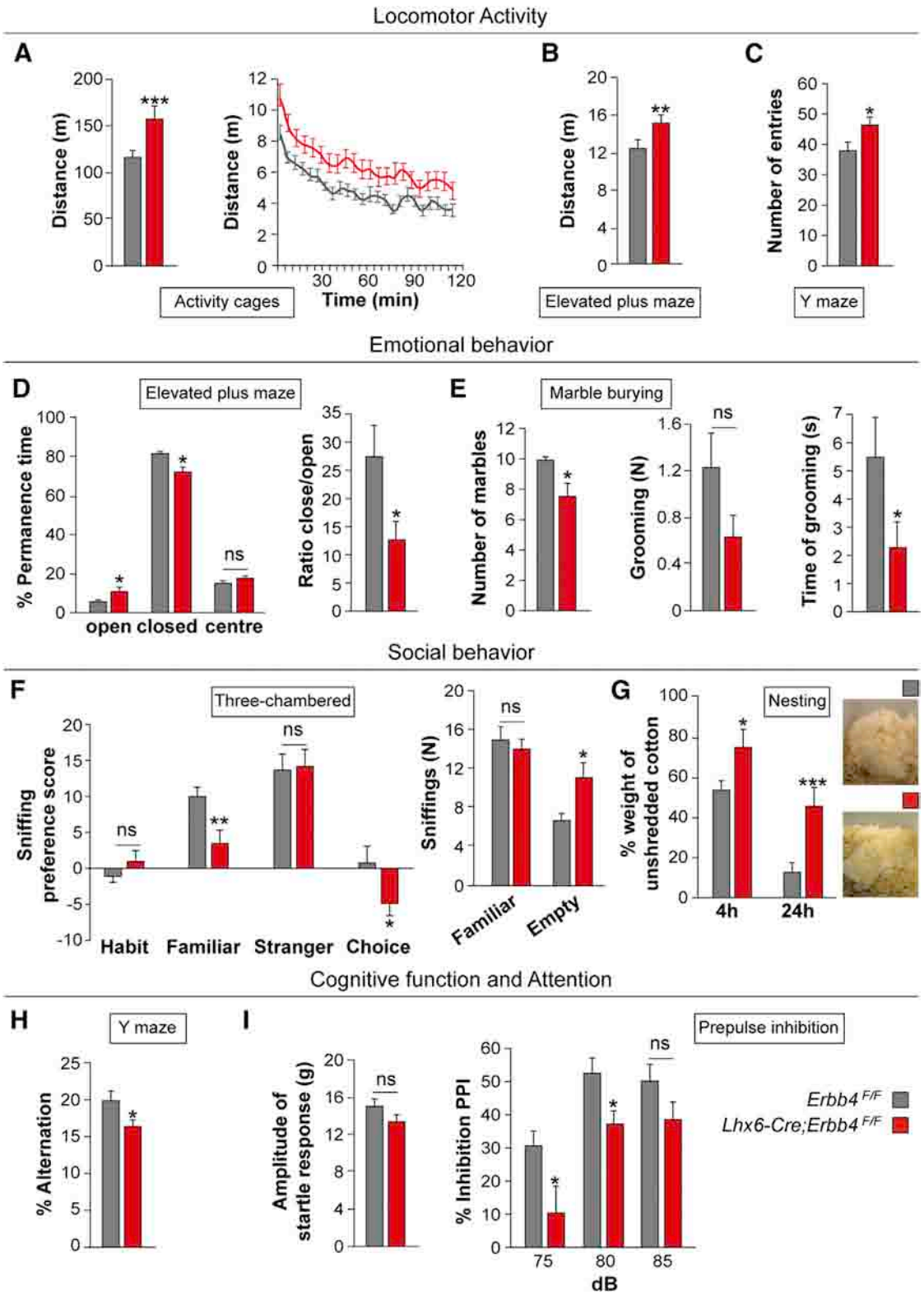

Figure 8. Early Conditional Deletion of *Erbb4* from Fast-Spiking Interneurons Causes Schizophrenia-Related Behaviors

(A–C) Locomotor activity of control and mutant mice. n = 15 control and 16 mutant mice in all experiments in this figure. (A) Locomotor activity in home cages. Left panel represents total distance, right panel shows a similar habituation curve. ***$p < 0.001$, t test. (B) Total distance in the plus maze. **$p < 0.01$, t test. (C) Total number of arm entries performed in the Y-maze. *$p < 0.05$, t test.

(legend continued on next page)

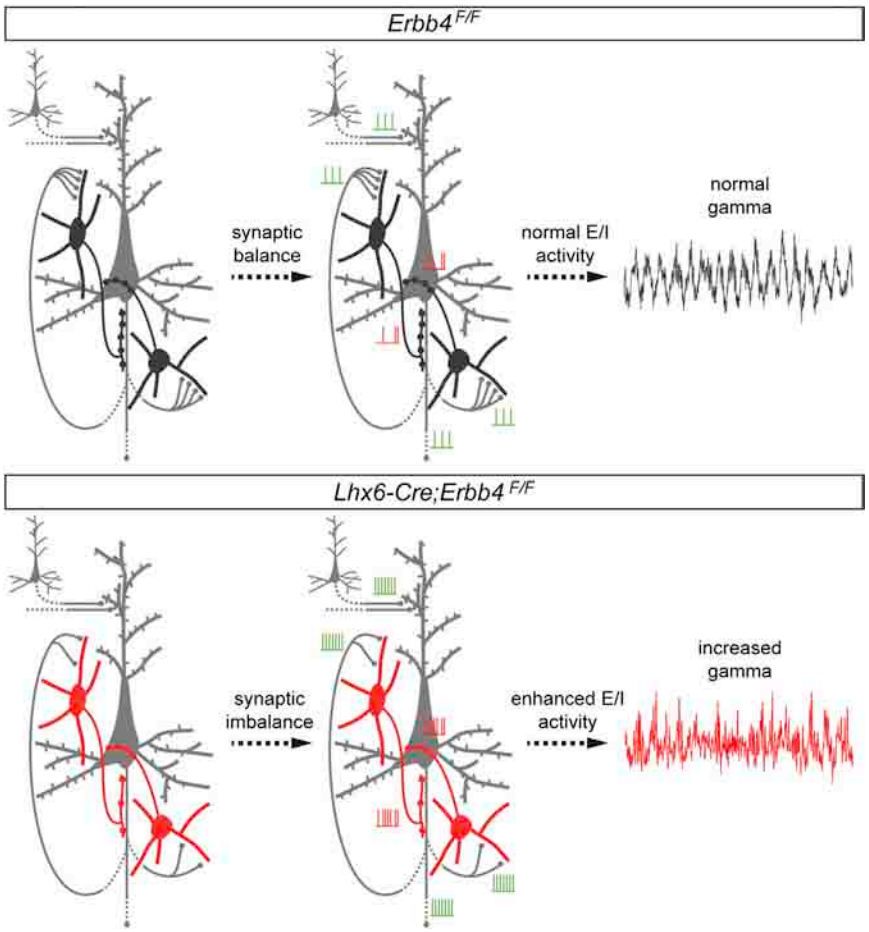

Figure 9. Summary of Alterations in Conditional *Erbb4* Mutants

During normal development, a synaptic balance between excitation and inhibition is reached in which fast-spiking interneurons (dark gray) shape the activity of the pyramidal cells (light gray) and synchronize their activity in the gamma band. In conditional *Erbb4* mutants, synaptic defects in fast-spiking interneurons cause an alteration in the excitatory/inhibitory balance, which eventually leads to a net increase in the activity of both pyramidal cells and fast-spiking interneurons. As a consequence, baseline gamma oscillations are abnormally increased and conditional *Erbb4* mutants display atypical behaviors.

See also Figure S1.

2006; Rico and Marín, 2011), our experiments, along with previous findings, strongly point to the abnormal function of fast-spiking interneurons as a primary cause in the pathogenesis of the disease.

ErbB4 Function in Synaptic Development

We, and others, have previously shown that fast-spiking interneurons require ErbB4 to receive a normal complement of glutamatergic synapses (Fazzari et al., 2010; Ting et al., 2011). In this study, we carried out cell-autonomous experiments to reveal that ErbB4 is similarly required for the development of excitatory inputs in the two main classes of fast-spiking interneurons, chandelier and basket cells. ErbB4 localizes to the postsynaptic density of glutamatergic terminals (Fazzari et al., 2010), where it interacts with synaptic clustering proteins such as PSD-95 (Garcia et al., 2000; Huang et al., 2000). NRG1-mediated activation of ErbB4 prevents the degradation of PSD-95, perhaps through its stabilization at the synapse (Ting et al., 2011). Thus, it seems plausible that ErbB4 may contribute to the formation of glutamatergic inputs to fast-spiking interneurons, at least in part, by enhancing the clustering of PSD-95.

ErbB4 appears to play divergent roles at presynaptic terminals in chandelier and basket cells. In the absence of ErbB4, the number of synapses made by chandelier cells onto the AIS of pyramidal cells is reduced (Fazzari et al., 2010; this study). In contrast, ErbB4 function does not seem to be required for the development of fast-spiking basket cell synapses, at least in the hippocampus. This suggests that loss of *Erbb4* might be more deleterious in cortical areas containing a relatively high density of chandelier cells, such as the hippocampus and entorhinal cortex (Inda et al., 2009), than in others.

Cortical Network Alterations in Conditional *Erbb4* Mutants

The analysis of the activity of pyramidal cells and interneurons in the hippocampus of conditional *Erbb4* mutants exposes the

(D and E) Emotional behavior of control and mutant mice. (D) Permanence in the different zones of the plus maze (expressed as percentage) and ratio of the time spent in the closed versus the open arms. *p < 0.05; t test. (E) Number of buried marbles, grooming episodes, and time grooming in the marble-burying test. *p < 0.05; t test.

(F and G) Social behavior in control and mutant mice. (F) Sniffing during habituation ("Habit": both cylinders empty), social phase with a familiar subject ("Familiar": familiar subject versus empty cylinder), social phase with an unfamiliar subject, ("Stranger": unfamiliar subject versus empty cylinder), preference for social novelty test ("Choice": familiar versus unfamiliar subject), and exposure to the familiar subject. **p < 0.01,*p < 0.05; two-way repeated-measures ANOVA with Bonferroni test as post hoc. (G) Nest building in control and mutant mice. Illustrative images of a nest built after 24 hr. ***p < 0.001, *p < 0.05, t test.

(H and I) Cognitive function in control and mutant mice. (H) Percentage of spontaneous alternation in the Y-maze. *p < 0.05, t test. (I) Baseline startle response to auditory-evoked startle stimulus (120 dB). *p < 0.05; t test. Percentage of prepulse inhibition of the auditory startle reflex across different prepulse intensities. *p < 0.05, t test.

See also Figures S1 and S8.

enormous plasticity of cortical networks. Deletion of ErbB4 from fast-spiking interneurons causes a partial cell-autonomous disconnection of these neurons from the cortical network that could be interpreted as a "hypo-GABAergic" phenotype. This initial deficit in GABAergic function leads to a prominent increase in the activity of pyramidal cells, which the network tries to accommodate by increasing the activity of interneurons through a homeostatic mechanism. As a consequence, the activity of both pyramidal cells and fast-spiking interneurons is boosted and the network seems to regain a certain balance, but operating at a much higher regime. This interpretation implies that network activity changes are secondary to the synaptic defects caused by the loss of ErbB4. Alternatively, it is at least theoretically possible that the observed synaptic deficits might be secondary to changes in the activity of fast-spiking interneurons. Consistent with this idea, ErbB4 seems to modulate the excitability of fast-spiking interneurons by inhibiting the activity of the voltage-gated potassium channel Kv1.1 (Li et al., 2012). Because Kv1.1 channels provide a gating mechanisms to fast-spiking interneurons (Goldberg et al., 2008), loss of ErbB4 in these cells could decrease their effectiveness in controlling the activity of pyramidal cells. However, the expression of Kv1.1 channels in fast-spiking interneurons does not reach its maturity until P18 (Goldberg et al., 2011), whereas interneurons have synaptic deficits as early as P15 (data not shown). Moreover, our viral deletion experiments strongly suggest that loss of ErbB4 causes cell-autonomous synaptic defects in the absence of network alterations. Our interpretation is also supported by computational models predicting similar alterations in network activity following relatively minor changes in the synaptic wiring of specific populations of interneurons (Cano-Colino and Compte, 2012; Loh et al., 2007).

Our analysis of cortical rhythms in conditional *Erbb4* mutants reveals a prominent boost in oscillatory activity in the hippocampus, together with a long-range decorrelation between cortical areas. In the hippocampus of anesthetized mice, increased power was observed for all frequencies above 4 Hz, including theta- and gamma-band oscillations, whereas only gamma-band oscillations were increased in freely moving conditional *Erbb4* mutants. This suggests that conditional *Erbb4* mutants might be particularly sensitive to the synchronizing activity of anesthesia at relatively slow frequencies. The increase in gamma band oscillations in the cortex of conditional *Erbb4* mutants is consistent with the observed enhancement in the activity of fast-spiking interneurons, through which gamma oscillations are generated (Cardin et al., 2009; Sohal et al., 2009; Wang and Buzsáki, 1996).

ErbB4 Signaling and Schizophrenia

Multiple lines of evidence indicate that GABAergic neurotransmission is disrupted in schizophrenia (Lewis et al., 2005; Sullivan and O'Donnell, 2012). The cellular basis for this alteration is unclear, but it may involve deficits in the phasic activation of interneurons, synthesis of GABA, and/or formation of inhibitory synapses. Remarkably, mouse mutants lacking *Erbb4* in fast-spiking interneurons develop deficits in all these three variables. In addition, our results reveal that a reduction in spine density in pyramidal cells, as described in schizophrenia (Glausier and Lewis, 2012), might be secondary to cell-autonomous defects in fast-spiking interneurons.

There is no direct evidence that fast-spiking interneurons receive less excitatory synapses in schizophrenia. However, it has been shown that NMDA receptor antagonists, such as ketamine, induce symptoms in adult healthy volunteers that are very similar to those of schizophrenia (Moghaddam and Krystal, 2012). NMDA receptor antagonists increase the excitability of pyramidal cells through a mechanism that may involve a reduction in the excitatory drive onto fast-spiking interneurons (Di Lazzaro et al., 2003; Homayoun and Moghaddam, 2007; Suzuki et al., 2002). These observations suggest that reduced excitation of fast-spiking interneurons may lead to an overall increase in network activity, as observed in conditional *Erbb4* mutants and that this might be a plausible component of the disease process in schizophrenia.

Decreased cortical *mRNA* expression of the GABA synthesizing enzyme GAD67 is one of the most replicated findings in schizophrenia postmortem brain studies (Akbarian et al., 1995; Duncan et al., 2010; Guidotti et al., 2000; Volk et al., 2000). Loss of GAD67 seems to preferentially affect fast-spiking interneurons (Curley et al., 2011; Hashimoto et al., 2003), which also contain reduced levels of PV (Hashimoto et al., 2003). Postmortem studies also revealed a reduction of GAT-1 in schizophrenia (Volk et al., 2002; Woo et al., 1998), whereas GAD65 levels seem unaffected (Guidotti et al., 2000; Hashimoto et al., 2008). Conditional deletion of *Erbb4* from these interneurons reproduces these deficits in mice, which reinforces the notion that ErbB4 is directly required to maintain normal levels of inhibition in the cortex. Intriguingly, common genetic variation in *ERBB4* also influences the concentration of GABA in the human cortex and cerebrospinal fluid (Luykx et al., 2012; Marenco et al., 2011).

Cortical Rhythms and Cognitive Impairment

Multiple lines of evidence suggest that gamma-band oscillations are reduced during the execution of cognitive tasks in schizophrenia (Haenschel et al., 2009; Hirano et al., 2008; Spencer et al., 2003; Uhlhaas et al., 2006). However, recent studies indicate that medication-naive, first-episode, and chronic patients with schizophrenia show elevated gamma-band power in resting state (Kikuchi et al., 2011; Spencer, 2011). Thus, cortical rhythm abnormalities in schizophrenia seem to include abnormal increases in baseline power as well as deficits in task-related oscillations (Uhlhaas and Singer, 2012).

Baseline increases in gamma oscillations are consistent with increases in the excitatory/inhibitory ratio of neurons (Yizhar et al., 2011), as observed here in conditional *Erbb4* mutants. Consistently, loss of NR1 receptors from PV+ interneurons leads to increased gamma-band oscillations in both anesthetized and behaving mice (Carlén et al., 2012; Korotkova et al., 2010). Remarkably, deletion of NR1 in PV+ interneurons also results in a significant reduction of theta oscillations (Carlén et al., 2012; Korotkova et al., 2010), which reflects the cellular specificity of both models.

Abnormal coupling between the hippocampus and the prefrontal cortex have been observed in schizophrenia patients (Ford et al., 2002; Heckers et al., 1998; Lawrie et al., 2002; Meyer-Lindenberg et al., 2005). Mice carrying the 22q11.2

microdeletion, a mutation associated with high risk for schizophrenia, also show disrupted synchrony between the hippocampus and the prefrontal cortex (Sigurdsson et al., 2010). Our current findings, which reveal abnormal hippocampal-prefrontal synchrony in conditional *Erbb4* mutants, reinforce the notion that genetic susceptibility to schizophrenia is strongly linked to deficient functional connectivity between temporal and frontal regions of the cortex.

Finally, impaired synchrony between the hippocampus and prefrontal cortex is associated with working memory deficits (Sigurdsson et al., 2010), as shown here in *Lhx6-Cre;Erbb4*$^{F/F}$ mutants. Working memory deficits have been previously observed in nervous system-specific *Erbb4* mice and in *PV*^{Cre}*;Erbb4*$^{F/F}$ conditional mutants (Golub et al., 2004; Wen et al., 2010), which suggest that impaired function of fast-spiking interneurons is associated with these defects. Beyond cognition, loss of *Erbb4* from fast-spiking interneurons also impacts many different aspects of behavior that have been previously associated with schizophrenia.

EXPERIMENTAL PROCEDURES

Mice

Lhx6-Cre;Erbb4$^{F/F}$ mice were generated by breeding *Lhx6-Cre* mice (Fogarty et al., 2007) with mice carrying loxP-flanked (F) *Erbb4* alleles (Golub et al., 2004) and sometimes with Rosa26 Reporter CAG-boosted EGFP (*RCE*) mice (Sousa et al., 2009). For most experiments, controls include mice carrying wild-type and *Lhx6-Cre* alleles. Animal procedures were approved by ethical committees (IN-CSIC and CEEA-PRBB) in accordance with Spanish (law 32/2007) and European regulations (EU directive 86/609, EU decree 2001-486).

Immunohistochemistry and Biochemistry

Immunohistochemistry was performed in 40–160 μm thick sections, as described previously (Fazzari et al., 2010). Cortical lysates were prepared from P30 control and *Lhx6-Cre;Erbb4*$^{F/F}$ mutants as described before (Fazzari et al., 2010).

In Utero Retroviral Infection and Electroporation

We performed in utero retroviral infections in the MGE of E14.5 *Erbb4*$^{F/F}$ using an ultrasound back-scattered microscope (Visualsonic), as described previously (Fazzari et al., 2010). In utero electroporation of the hippocampus was performed using an electroporator (CUY21E, Nepa GENE) as described before (Chacón et al., 2012).

Image Acquisition and Analysis

We used Neurolucida for cell density, colocalization, chandelier candlesticks, and spine counting. For the analysis of presynaptic and postsynaptic markers, images were acquired and quantified as described before (Fazzari et al., 2010).

In Vitro Patch Clamp Recordings

Electrophysiological recordings were carried out at postnatal day (P) 20–22 on sagittal slices.

In Vivo Recordings on Anesthetized Mice

Two- to 3-month-old male mice were anesthetized with intraperitoneal injections of urethane or ketamine/xylazine. Craniotomies were performed and linear Michigan probes (32 channel, NeuroNexus Technologies) for field potential recordings were inserted in the dorsal hippocampus and prefrontal cortex of the same brain hemisphere.

In Vivo Recordings on Freely Moving Mice

Microdrives (Axona) with four or eight independent screws were loaded with tetrodes and implanted through a craniotomy above the hippocampus under isoflurane anesthesia and buprenorphine analgesia. Electrophysiological recordings were performed as described before (Brotons-Mas et al., 2010).

Electrophysiological Analysis

In anesthetized and freely moving mice, signal processing was performed off-line by custom-written MATLAB code (MathWorks).

Behavioral Analyses

For behavioral testing, we used a specifically adapted battery to capture disease-specific phenotypes expressed upon *Erbb4* ablation.

SUPPLEMENTAL INFORMATION

Supplemental Information includes Supplemental Experimental Procedures, eight figures, and one table and can be found with this article online at http://dx.doi.org/10.1016/j.neuron.2013.07.010.

ACKNOWLEDGMENTS

We thank D. Baeza and M. Fernández-Otero for excellent technical assistance, A. Casillas, T. Gil, and M. Pérez for general laboratory support, G. Fishell (New York University), K. Lloyd (University College Dublin), and N. Kessaris (University College London) for *RCE*, *Erbb4*, and *Lhx6-Cre* mouse strains, respectively, and J-M. Fritschy (University of Zurich) for GABA receptor antibodies. We are also grateful to members of the Borrell, Marín, and Rico laboratories for stimulating discussions and ideas. Supported by grants from the Spanish Government to B.R. (SAF2010-21723 and CONSOLIDER CSD2007-00023), O.M. (CSD2007-00023), M.D. (SAF2010-16427), and S.C. (CSD2007-00023, BFU2009-09938 and PIM2010ERN-00679, part of the ERANET NEURON TRANSALC project), from Fundación Alicia Koplowitz to B.R., from the Lilly Research Awards Program to B.R. and O.M., and from Fundació la Marató to O.M., B.R., and M.D. B.R. is an EMBO Young Investigator.

Accepted: July 5, 2013
Published: September 18, 2013

REFERENCES

Akbarian, S., Kim, J.J., Potkin, S.G., Hagman, J.O., Tafazzoli, A., Bunney, W.E., Jr., and Jones, E.G. (1995). Gene expression for glutamic acid decarboxylase is reduced without loss of neurons in prefrontal cortex of schizophrenics. Arch. Gen. Psychiatry *52*, 258–266.

Allen, N.C., Bagade, S., McQueen, M.B., Ioannidis, J.P., Kavvoura, F.K., Khoury, M.J., Tanzi, R.E., and Bertram, L. (2008). Systematic meta-analyses and field synopsis of genetic association studies in schizophrenia: the SzGene database. Nat. Genet. *40*, 827–834.

Brotons-Mas, J.R., Montejo, N., O'Mara, S.M., and Sánchez-Vives, M.V. (2010). Stability of subicular place fields across multiple light and dark transitions. Eur. J. Neurosci. *32*, 648–658.

Buzsáki, G., and Draguhn, A. (2004). Neuronal oscillations in cortical networks. Science *304*, 1926–1929.

Cano-Colino, M., and Compte, A. (2012). A computational model for spatial working memory deficits in schizophrenia. Pharmacopsychiatry *45*(*Suppl 1*), S49–S56.

Cardin, J.A., Carlén, M., Meletis, K., Knoblich, U., Zhang, F., Deisseroth, K., Tsai, L.H., and Moore, C.I. (2009). Driving fast-spiking cells induces gamma rhythm and controls sensory responses. Nature *459*, 663–667.

Carlén, M., Meletis, K., Siegle, J.H., Cardin, J.A., Futai, K., Vierling-Claassen, D., Rühlmann, C., Jones, S.R., Deisseroth, K., Sheng, M., et al. (2012). A critical role for NMDA receptors in parvalbumin interneurons for gamma rhythm induction and behavior. Mol. Psychiatry *17*, 537–548.

Chacón, M.R., Navarro, A.I., Cuesto, G., del Pino, I., Scott, R., Morales, M., and Rico, B. (2012). Focal adhesion kinase regulates actin nucleation and neuronal filopodia formation during axonal growth. Development *139*, 3200–3210.

Chattopadhyaya, B., Di Cristo, G., Wu, C.Z., Knott, G., Kuhlman, S., Fu, Y., Palmiter, R.D., and Huang, Z.J. (2007). GAD67-mediated GABA synthesis and signaling regulate inhibitory synaptic innervation in the visual cortex. Neuron *54*, 889–903.

Chen, P.L., Avramopoulos, D., Lasseter, V.K., McGrath, J.A., Fallin, M.D., Liang, K.Y., Nestadt, G., Feng, N., Steel, G., Cutting, A.S., et al. (2009). Fine mapping on chromosome 10q22-q23 implicates Neuregulin 3 in schizophrenia. Am. J. Hum. Genet. *84*, 21–34.

Curley, A.A., and Lewis, D.A. (2012). Cortical basket cell dysfunction in schizophrenia. J. Physiol. *590*, 715–724.

Curley, A.A., Arion, D., Volk, D.W., Asafu-Adjei, J.K., Sampson, A.R., Fish, K.N., and Lewis, D.A. (2011). Cortical deficits of glutamic acid decarboxylase 67 expression in schizophrenia: clinical, protein, and cell type-specific features. Am. J. Psychiatry *168*, 921–929.

Di Lazzaro, V., Oliviero, A., Profice, P., Pennisi, M.A., Pilato, F., Zito, G., Dileone, M., Nicoletti, R., Pasqualetti, P., and Tonali, P.A. (2003). Ketamine increases human motor cortex excitability to transcranial magnetic stimulation. J. Physiol. *547*, 485–496.

Duncan, C.E., Webster, M.J., Rothmond, D.A., Bahn, S., Elashoff, M., and Shannon Weickert, C. (2010). Prefrontal GABA(A) receptor alpha-subunit expression in normal postnatal human development and schizophrenia. J. Psychiatr. Res. *44*, 673–681.

Fazzari, P., Paternain, A.V., Valiente, M., Pla, R., Luján, R., Lloyd, K., Lerma, J., Marín, O., and Rico, B. (2010). Control of cortical GABA circuitry development by Nrg1 and ErbB4 signalling. Nature *464*, 1376–1380.

Flames, N., Long, J.E., Garratt, A.N., Fischer, T.M., Gassmann, M., Birchmeier, C., Lai, C., Rubenstein, J.L., and Marín, O. (2004). Short- and long-range attraction of cortical GABAergic interneurons by neuregulin-1. Neuron *44*, 251–261.

Flames, N., Pla, R., Gelman, D.M., Rubenstein, J.L., Puelles, L., and Marín, O. (2007). Delineation of multiple subpallial progenitor domains by the combinatorial expression of transcriptional codes. J. Neurosci. *27*, 9682–9695.

Fogarty, M., Grist, M., Gelman, D., Marín, O., Pachnis, V., and Kessaris, N. (2007). Spatial genetic patterning of the embryonic neuroepithelium generates GABAergic interneuron diversity in the adult cortex. J. Neurosci. *27*, 10935–10946.

Ford, J.M., Mathalon, D.H., Whitfield, S., Faustman, W.O., and Roth, W.T. (2002). Reduced communication between frontal and temporal lobes during talking in schizophrenia. Biol. Psychiatry *51*, 485–492.

Garcia, R.A., Vasudevan, K., and Buonanno, A. (2000). The neuregulin receptor ErbB-4 interacts with PDZ-containing proteins at neuronal synapses. Proc. Natl. Acad. Sci. USA *97*, 3596–3601.

Gelman, D., Griveau, A., Dehorter, N., Teissier, A., Varela, C., Pla, R., Pierani, A., and Marín, O. (2011). A wide diversity of cortical GABAergic interneurons derives from the embryonic preoptic area. J. Neurosci. *31*, 16570–16580.

Glausier, J.R., and Lewis, D.A. (2012). Dendritic spine pathology in schizophrenia. Neuroscience. Published online April 27, 2012. http://dx.doi.org/10.1016/j.neuroscience.2012.04.044.

Goldberg, E.M., Clark, B.D., Zagha, E., Nahmani, M., Erisir, A., and Rudy, B. (2008). K+ channels at the axon initial segment dampen near-threshold excitability of neocortical fast-spiking GABAergic interneurons. Neuron *58*, 387–400.

Goldberg, E.M., Jeong, H.Y., Kruglikov, I., Tremblay, R., Lazarenko, R.M., and Rudy, B. (2011). Rapid developmental maturation of neocortical FS cell intrinsic excitability. Cereb. Cortex *21*, 666–682.

Golub, M.S., Germann, S.L., and Lloyd, K.C. (2004). Behavioral characteristics of a nervous system-specific erbB4 knock-out mouse. Behav. Brain Res. *153*, 159–170.

Guidotti, A., Auta, J., Davis, J.M., Di-Giorgi-Gerevini, V., Dwivedi, Y., Grayson, D.R., Impagnatiello, F., Pandey, G., Pesold, C., Sharma, R., et al. (2000). Decrease in reelin and glutamic acid decarboxylase67 (GAD67) expression in schizophrenia and bipolar disorder: a postmortem brain study. Arch. Gen. Psychiatry *57*, 1061–1069.

Haenschel, C., Bittner, R.A., Waltz, J., Haertling, F., Wibral, M., Singer, W., Linden, D.E., and Rodriguez, E. (2009). Cortical oscillatory activity is critical for working memory as revealed by deficits in early-onset schizophrenia. J. Neurosci. *29*, 9481–9489.

Harrison, P.J., and Law, A.J. (2006). Neuregulin 1 and schizophrenia: genetics, gene expression, and neurobiology. Biol. Psychiatry *60*, 132–140.

Hashimoto, T., Volk, D.W., Eggan, S.M., Mirnics, K., Pierri, J.N., Sun, Z., Sampson, A.R., and Lewis, D.A. (2003). Gene expression deficits in a subclass of GABA neurons in the prefrontal cortex of subjects with schizophrenia. J. Neurosci. *23*, 6315–6326.

Hashimoto, T., Arion, D., Unger, T., Maldonado-Avilés, J.G., Morris, H.M., Volk, D.W., Mirnics, K., and Lewis, D.A. (2008). Alterations in GABA-related transcriptome in the dorsolateral prefrontal cortex of subjects with schizophrenia. Mol. Psychiatry *13*, 147–161.

Heckers, S., Rauch, S.L., Goff, D., Savage, C.R., Schacter, D.L., Fischman, A.J., and Alpert, N.M. (1998). Impaired recruitment of the hippocampus during conscious recollection in schizophrenia. Nat. Neurosci. *1*, 318–323.

Hirano, S., Hirano, Y., Maekawa, T., Obayashi, C., Oribe, N., Kuroki, T., Kanba, S., and Onitsuka, T. (2008). Abnormal neural oscillatory activity to speech sounds in schizophrenia: a magnetoencephalography study. J. Neurosci. *28*, 4897–4903.

Homayoun, H., and Moghaddam, B. (2007). NMDA receptor hypofunction produces opposite effects on prefrontal cortex interneurons and pyramidal neurons. J. Neurosci. *27*, 11496–11500.

Huang, Z.J., Kirkwood, A., Pizzorusso, T., Porciatti, V., Morales, B., Bear, M.F., Maffei, L., and Tonegawa, S. (1999). BDNF regulates the maturation of inhibition and the critical period of plasticity in mouse visual cortex. Cell *98*, 739–755.

Huang, Y.Z., Won, S., Ali, D.W., Wang, Q., Tanowitz, M., Du, Q.S., Pelkey, K.A., Yang, D.J., Xiong, W.C., Salter, M.W., and Mei, L. (2000). Regulation of neuregulin signaling by PSD-95 interacting with ErbB4 at CNS synapses. Neuron *26*, 443–455.

Inda, M.C., DeFelipe, J., and Muñoz, A. (2009). Morphology and distribution of chandelier cell axon terminals in the mouse cerebral cortex and claustroamygdaloid complex. Cereb. Cortex *19*, 41–54.

Insel, T.R. (2010). Rethinking schizophrenia. Nature *468*, 187–193.

Jensen, O., Kaiser, J., and Lachaux, J.P. (2007). Human gamma-frequency oscillations associated with attention and memory. Trends Neurosci. *30*, 317–324.

Kao, W.T., Wang, Y., Kleinman, J.E., Lipska, B.K., Hyde, T.M., Weinberger, D.R., and Law, A.J. (2010). Common genetic variation in Neuregulin 3 (NRG3) influences risk for schizophrenia and impacts NRG3 expression in human brain. Proc. Natl. Acad. Sci. USA *107*, 15619–15624.

Kikuchi, M., Hashimoto, T., Nagasawa, T., Hirosawa, T., Minabe, Y., Yoshimura, M., Strik, W., Dierks, T., and Koenig, T. (2011). Frontal areas contribute to reduced global coordination of resting-state gamma activities in drug-naïve patients with schizophrenia. Schizophr. Res. *130*, 187–194.

Korotkova, T., Fuchs, E.C., Ponomarenko, A., von Engelhardt, J., and Monyer, H. (2010). NMDA receptor ablation on parvalbumin-positive interneurons impairs hippocampal synchrony, spatial representations, and working memory. Neuron *68*, 557–569.

Lavdas, A.A., Grigoriou, M., Pachnis, V., and Parnavelas, J.G. (1999). The medial ganglionic eminence gives rise to a population of early neurons in the developing cerebral cortex. J. Neurosci. *19*, 7881–7888.

Lawrie, S.M., Buechel, C., Whalley, H.C., Frith, C.D., Friston, K.J., and Johnstone, E.C. (2002). Reduced frontotemporal functional connectivity in schizophrenia associated with auditory hallucinations. Biol. Psychiatry *51*, 1008–1011.

Lewis, D.A. (2011). The chandelier neuron in schizophrenia. Dev. Neurobiol. *71*, 118–127.

Lewis, D.A., and Sweet, R.A. (2009). Schizophrenia from a neural circuitry perspective: advancing toward rational pharmacological therapies. J. Clin. Invest. *119*, 706–716.

Lewis, D.A., Cruz, D.A., Melchitzky, D.S., and Pierri, J.N. (2001). Lamina-specific deficits in parvalbumin-immunoreactive varicosities in the prefrontal cortex of subjects with schizophrenia: evidence for fewer projections from the thalamus. Am. J. Psychiatry *158*, 1411–1422.

Lewis, D.A., Hashimoto, T., and Volk, D.W. (2005). Cortical inhibitory neurons and schizophrenia. Nat. Rev. Neurosci. *6*, 312–324.

Li, K.X., Lu, Y.M., Xu, Z.H., Zhang, J., Zhu, J.M., Zhang, J.M., Cao, S.X., Chen, X.J., Chen, Z., Luo, J.H., et al. (2012). Neuregulin 1 regulates excitability of fast-spiking neurons through Kv1.1 and acts in epilepsy. Nat. Neurosci. *15*, 267–273.

Lisman, J.E., Coyle, J.T., Green, R.W., Javitt, D.C., Benes, F.M., Heckers, S., and Grace, A.A. (2008). Circuit-based framework for understanding neurotransmitter and risk gene interactions in schizophrenia. Trends Neurosci. *31*, 234–242.

Loh, M., Rolls, E.T., and Deco, G. (2007). A dynamical systems hypothesis of schizophrenia. PLoS Comput. Biol. *3*, e228.

Loup, F., Weinmann, O., Yonekawa, Y., Aguzzi, A., Wieser, H.G., and Fritschy, J.M. (1998). A highly sensitive immunofluorescence procedure for analyzing the subcellular distribution of GABAA receptor subunits in the human brain. J. Histochem. Cytochem. *46*, 1129–1139.

Luykx, J.J., Vinkers, C.H., Bakker, S.C., Visser, W.F., van Boxmeer, L., Strengman, E., van Eijk, K.R., Lens, J.A., Borgdorff, P., Keijzers, P., et al. (2012). A common variant in ERBB4 regulates GABA concentrations in human cerebrospinal fluid. Neuropsychopharmacology *37*, 2088–2092.

Marenco, S., Geramita, M., van der Veen, J.W., Barnett, A.S., Kolachana, B., Shen, J., Weinberger, D.R., and Law, A.J. (2011). Genetic association of ErbB4 and human cortical GABA levels in vivo. J. Neurosci. *31*, 11628–11632.

Mei, L., and Xiong, W.C. (2008). Neuregulin 1 in neural development, synaptic plasticity and schizophrenia. Nat. Rev. Neurosci. *9*, 437–452.

Meyer-Lindenberg, A.S., Olsen, R.K., Kohn, P.D., Brown, T., Egan, M.F., Weinberger, D.R., and Berman, K.F. (2005). Regionally specific disturbance of dorsolateral prefrontal-hippocampal functional connectivity in schizophrenia. Arch. Gen. Psychiatry *62*, 379–386.

Minzenberg, M.J., and Carter, C.S. (2012). Developing treatments for impaired cognition in schizophrenia. Trends Cogn. Sci. *16*, 35–42.

Moghaddam, B., and Krystal, J.H. (2012). Capturing the angel in "angel dust": twenty years of translational neuroscience studies of NMDA receptor antagonists in animals and humans. Schizophr. Bull. *38*, 942–949.

Morar, B., Dragović, M., Waters, F.A., Chandler, D., Kalaydjieva, L., and Jablensky, A. (2011). Neuregulin 3 (NRG3) as a susceptibility gene in a schizophrenia subtype with florid delusions and relatively spared cognition. Mol. Psychiatry *16*, 860–866.

Mulle, J.G. (2012). Schizophrenia genetics: progress, at last. Curr. Opin. Genet. Dev. *22*, 238–244.

Neddens, J., and Buonanno, A. (2010). Selective populations of hippocampal interneurons express ErbB4 and their number and distribution is altered in ErbB4 knockout mice. Hippocampus *20*, 724–744.

Neddens, J., Fish, K.N., Tricoire, L., Vullhorst, D., Shamir, A., Chung, W., Lewis, D.A., McBain, C.J., and Buonanno, A. (2011). Conserved interneuron-specific ErbB4 expression in frontal cortex of rodents, monkeys, and humans: implications for schizophrenia. Biol. Psychiatry *70*, 636–645.

Nicodemus, K.K., Luna, A., Vakkalanka, R., Goldberg, T., Egan, M., Straub, R.E., and Weinberger, D.R. (2006). Further evidence for association between ErbB4 and schizophrenia and influence on cognitive intermediate phenotypes in healthy controls. Mol. Psychiatry *11*, 1062–1065.

Norton, N., Moskvina, V., Morris, D.W., Bray, N.J., Zammit, S., Williams, N.M., Williams, H.J., Preece, A.C., Dwyer, S., Wilkinson, J.C., et al. (2006). Evidence that interaction between neuregulin 1 and its receptor erbB4 increases susceptibility to schizophrenia. Am. J. Med. Genet. B. Neuropsychiatr. Genet. *141B*, 96–101.

Nusser, Z., Sieghart, W., Benke, D., Fritschy, J.M., and Somogyi, P. (1996). Differential synaptic localization of two major gamma-aminobutyric acid type A receptor alpha subunits on hippocampal pyramidal cells. Proc. Natl. Acad. Sci. USA *93*, 11939–11944.

Pratt, J., Winchester, C., Dawson, N., and Morris, B. (2012). Advancing schizophrenia drug discovery: optimizing rodent models to bridge the translational gap. Nat. Rev. Drug Discov. *11*, 560–579.

Rico, B., and Marín, O. (2011). Neuregulin signaling, cortical circuitry development and schizophrenia. Curr. Opin. Genet. Dev. *21*, 262–270.

Rymar, V.V., and Sadikot, A.F. (2007). Laminar fate of cortical GABAergic interneurons is dependent on both birthdate and phenotype. J. Comp. Neurol. *501*, 369–380.

Shamir, A., Kwon, O.B., Karavanova, I., Vullhorst, D., Leiva-Salcedo, E., Janssen, M.J., and Buonanno, A. (2012). The importance of the NRG-1/ErbB4 pathway for synaptic plasticity and behaviors associated with psychiatric disorders. J. Neurosci. *32*, 2988–2997.

Sigurdsson, T., Stark, K.L., Karayiorgou, M., Gogos, J.A., and Gordon, J.A. (2010). Impaired hippocampal-prefrontal synchrony in a genetic mouse model of schizophrenia. Nature *464*, 763–767.

Silberberg, G., Darvasi, A., Pinkas-Kramarski, R., and Navon, R. (2006). The involvement of ErbB4 with schizophrenia: association and expression studies. Am. J. Med. Genet. B. Neuropsychiatr. Genet. *141B*, 142–148.

Sohal, V.S., Zhang, F., Yizhar, O., and Deisseroth, K. (2009). Parvalbumin neurons and gamma rhythms enhance cortical circuit performance. Nature *459*, 698–702.

Sousa, V.H., Miyoshi, G., Hjerling-Leffler, J., Karayannis, T., and Fishell, G. (2009). Characterization of Nkx6-2-derived neocortical interneuron lineages. Cereb. Cortex *19*(*Suppl 1*), i1–i10.

Spencer, K.M. (2011). Baseline gamma power during auditory steady-state stimulation in schizophrenia. Front. Hum. Neurosci. *5*, 190.

Spencer, K.M., Nestor, P.G., Niznikiewicz, M.A., Salisbury, D.F., Shenton, M.E., and McCarley, R.W. (2003). Abnormal neural synchrony in schizophrenia. J. Neurosci. *23*, 7407–7411.

Stefansson, H., Sigurdsson, E., Steinthorsdottir, V., Bjornsdottir, S., Sigmundsson, T., Ghosh, S., Brynjolfsson, J., Gunnarsdottir, S., Ivarsson, O., Chou, T.T., et al. (2002). Neuregulin 1 and susceptibility to schizophrenia. Am. J. Hum. Genet. *71*, 877–892.

Sullivan, E.M., and O'Donnell, P. (2012). Inhibitory interneurons, oxidative stress, and schizophrenia. Schizophr. Bull. *38*, 373–376.

Sullivan, P.F., Daly, M.J., and O'Donovan, M. (2012). Genetic architectures of psychiatric disorders: the emerging picture and its implications. Nat. Rev. Genet. *13*, 537–551.

Suzuki, Y., Jodo, E., Takeuchi, S., Niwa, S., and Kayama, Y. (2002). Acute administration of phencyclidine induces tonic activation of medial prefrontal cortex neurons in freely moving rats. Neuroscience *114*, 769–779.

Ting, A.K., Chen, Y., Wen, L., Yin, D.M., Shen, C., Tao, Y., Liu, X., Xiong, W.C., and Mei, L. (2011). Neuregulin 1 promotes excitatory synapse development and function in GABAergic interneurons. J. Neurosci. *31*, 15–25.

Uhlhaas, P.J., and Singer, W. (2012). Neuronal dynamics and neuropsychiatric disorders: toward a translational paradigm for dysfunctional large-scale networks. Neuron *75*, 963–980.

Uhlhaas, P.J., Linden, D.E., Singer, W., Haenschel, C., Lindner, M., Maurer, K., and Rodriguez, E. (2006). Dysfunctional long-range coordination of neural activity during Gestalt perception in schizophrenia. J. Neurosci. *26*, 8168–8175.

Volk, D.W., Austin, M.C., Pierri, J.N., Sampson, A.R., and Lewis, D.A. (2000). Decreased glutamic acid decarboxylase67 messenger RNA expression in a subset of prefrontal cortical gamma-aminobutyric acid neurons in subjects with schizophrenia. Arch. Gen. Psychiatry *57*, 237–245.

Volk, D.W., Pierri, J.N., Fritschy, J.M., Auh, S., Sampson, A.R., and Lewis, D.A. (2002). Reciprocal alterations in pre- and postsynaptic inhibitory markers at chandelier cell inputs to pyramidal neurons in schizophrenia. Cereb. Cortex *12*, 1063–1070.

Walsh, T., McClellan, J.M., McCarthy, S.E., Addington, A.M., Pierce, S.B., Cooper, G.M., Nord, A.S., Kusenda, M., Malhotra, D., Bhandari, A., et al.

(2008). Rare structural variants disrupt multiple genes in neurodevelopmental pathways in schizophrenia. Science *320*, 539–543.

Wang, X.J., and Buzsáki, G. (1996). Gamma oscillation by synaptic inhibition in a hippocampal interneuronal network model. J. Neurosci. *16*, 6402–6413.

Wang, Y.C., Chen, J.Y., Chen, M.L., Chen, C.H., Lai, I.C., Chen, T.T., Hong, C.J., Tsai, S.J., and Liou, Y.J. (2008). Neuregulin 3 genetic variations and susceptibility to schizophrenia in a Chinese population. Biol. Psychiatry *64*, 1093–1096.

Wen, L., Lu, Y.S., Zhu, X.H., Li, X.M., Woo, R.S., Chen, Y.J., Yin, D.M., Lai, C., Terry, A.V., Jr., Vazdarjanova, A., et al. (2010). Neuregulin 1 regulates pyramidal neuron activity via ErbB4 in parvalbumin-positive interneurons. Proc. Natl. Acad. Sci. USA *107*, 1211–1216.

Woo, T.U., Whitehead, R.E., Melchitzky, D.S., and Lewis, D.A. (1998). A subclass of prefrontal gamma-aminobutyric acid axon terminals are selectively altered in schizophrenia. Proc. Natl. Acad. Sci. USA *95*, 5341–5346.

Woo, R.S., Li, X.M., Tao, Y., Carpenter-Hyland, E., Huang, Y.Z., Weber, J., Neiswender, H., Dong, X.P., Wu, J., Gassmann, M., et al. (2007). Neuregulin-1 enhances depolarization-induced GABA release. Neuron *54*, 599–610.

Yau, H.J., Wang, H.F., Lai, C., and Liu, F.C. (2003). Neural development of the neuregulin receptor ErbB4 in the cerebral cortex and the hippocampus: preferential expression by interneurons tangentially migrating from the ganglionic eminences. Cereb. Cortex *13*, 252–264.

Yizhar, O., Fenno, L.E., Prigge, M., Schneider, F., Davidson, T.J., O'Shea, D.J., Sohal, V.S., Goshen, I., Finkelstein, J., Paz, J.T., et al. (2011). Neocortical excitation/inhibition balance in information processing and social dysfunction. Nature *477*, 171–178.